SIAM J. Sci. Comput.
Vol. 38, No. 2, pp. B191–B218

A NEWTON-TYPE METHOD WITH NONEQUIVALENCE DEFLATION FOR NONLINEAR EIGENVALUE PROBLEMS ARISING IN PHOTONIC CRYSTAL MODELING[*]

TSUNG-MING HUANG[†], WEN-WEI LIN[‡], AND VOLKER MEHRMANN[§]

Abstract. The numerical simulation of the band structure of three-dimensional dispersive metallic photonic crystals with face-centered cubic lattices leads to large-scale nonlinear eigenvalue problems, which are very challenging due to a high-dimensional subspace associated with the eigenvalue zero and the fact that the desired eigenvalues (with smallest real part) cluster and are close to the zero eigenvalues. For the solution of the nonlinear eigenvalue problem, a Newton-type iterative method is proposed and the nullspace-free method is applied to exclude the zero eigenvalues from the associated generalized eigenvalue problem. To find the successive eigenvalue/eigenvector pairs, we propose a new nonequivalence deflation method to transform converged eigenvalues to infinity, while all other eigenvalues remain unchanged. The deflated problem is then solved by the same Newton-type method, which is used as a hybrid method that combines with the Jacobi–Davidson and the nonlinear Arnoldi methods to compute the clustering eigenvalues. Numerical results illustrate that the proposed method is robust even for the case of computing many clustering eigenvalues in very large problems.

Key words. Maxwell equation, dispersive metallic photonic crystals, nonlinear eigenvalue problem, Newton-type method, nonequivalence deflation, Jacobi–Davidson method, shift-invert residual Arnoldi method, nonlinear Arnoldi method

AMS subject classifications. 15A18, 15A90, 65F15

DOI. 10.1137/151004823

1. Introduction.

The electromagnetic wave propagation through dispersive metallic photonic crystals (PCs) has been extensively studied over the past few decades [8, 9, 10, 34, 38, 47]. A standard model for studying the electromagnetic effects in periodic structures and dispersive isotropic materials is the three-dimensional (3D) Maxwell equation

$$\nabla \times \nabla \times E(\mathbf{r}) = \omega^2 \varepsilon(\mathbf{r}, \omega) E(\mathbf{r}), \tag{1.1}$$

where $E(\mathbf{r})$ denotes the electric field at position $\mathbf{r} \in \mathbb{R}^3$ and

$$\varepsilon(\mathbf{r}, \omega) = \begin{cases} \varepsilon_d(\omega), & \mathbf{r} \text{ in the dispersive material domain,} \\ \varepsilon_n, & \mathbf{r} \text{ in the nondispersive material domain,} \end{cases}$$

denotes the permittivity, in which ε_n is a constant and $\varepsilon_d(\omega)$ is dependent on the frequency ω.

[*] Submitted to the journal's Computational Methods in Science and Engineering section January 20, 2015; accepted for publication (in revised form) January 5, 2016; published electronically March 15, 2016.

http://www.siam.org/journals/sisc/38-2/100482.html

[†] Department of Mathematics, National Taiwan Normal University, Taipei 116, Taiwan (min@ntnu.edu.tw). This author's work was partially supported by the Ministry of Science and Technology (MoST), National Centre of Theoretical Sciences (NCTS) in Taiwan.

[‡] Department of Applied Mathematics, National Chiao Tung University, Hsinchu 300, Taiwan (wwlin@math.nctu.edu.tw). This author's work was partially supported by MoST, NCTS, and the ST Yau Centre in Taiwan and by the DAAD "Deutscher Akademischer Austausch Dienst" in Germany.

[§] Institut für Mathematik, TU Berlin, D-10623 Berlin, Germany (mehrmann@math.tu-berlin.de). This author's research was carried out in the framework of Matheon project *D-OT3, Adaptive finite element methods for nonlinear parameter-dependent eigenvalue problems in photonic crystals*, supported by the Einstein Foundation Berlin.

In the Drude model of a dispersive material [34, 38, 52, 53], the permittivity $\varepsilon_d(\omega)$ is modeled as

$$\varepsilon_d(\omega) = 1 - \frac{\omega_p^2}{\omega^2 + \imath\Gamma_p\omega}, \tag{1.2}$$

where $\imath = \sqrt{-1}$, ω_p is a plasma frequency, and Γ_p is the corresponding damping frequency. The more involved Drude–Lorentz model [10, 11, 34, 47] uses the permittivity model

$$\varepsilon_d(\omega) = \varepsilon_\infty - \frac{\omega_p^2}{\omega^2 + \imath\Gamma_p\omega} + \sum_{j=1}^{2} \Omega_j A_j \left(\frac{e^{\imath\phi_j}}{\Omega_j - \omega - \imath\Gamma_j} + \frac{e^{-\imath\phi_j}}{\Omega_j + \omega + \imath\Gamma_j} \right), \tag{1.3}$$

where ε_∞ is a high-frequency limit dielectric constant, and ϕ_j, Ω_j, A_j, and Γ_j are the parameters for the two pairs of poles in the Lorentz model. The first and second terms in (1.3) correspond to the contributions of a Drude model with $\varepsilon_\infty = 1$. The third term arises from the interband transitions.

There are many approaches for the numerical simulation of wave propagation in PCs. Very often, time-domain simulation methods (see, e.g., [12]) are used to calculate the band structures of 3D metallic PCs, but in order to obtain reasonable results, extremely long simulation times are required. As an alternative, often the Fourier transform and the discretization of the time-invariant system (1.1) are considered, which lead to a nonlinear eigenvalue problem (NLEVP) [8, 9, 34] rational in the frequency ω. To solve large-scale NLEVPs, however, is also a nontrivial task [37, 46] and is particularly challenging for 3D metallic PCs. In [8, 9, 34], the rational eigenvalue problem is reformulated as a polynomial eigenvalue problem (PEP) by multiplying with the common denominator. The PEP is then reformulated (linearized) [13, 35] as a generalized eigenvalue problem to which standard eigenvalue methods [2, 32, 39] can be applied. However, in this approach the order of the problem is highly enlarged and the sensitivity of the eigenvalues and eigenvectors may increase considerably, since the set of admissible perturbations for the linearized eigenvalue problem is larger than that of the PEP [45] and even larger than that of the rational problem.

A completely different eigenvalue method is to work directly with the NLEVP. One can use the polynomial Jacobi–Davidson method [21, 24, 41, 42, 50] for the PEPs or the rational Krylov method [26, 40], the nonlinear Arnoldi method [48], the nonlinear Jacobi–Davidson method [49], contour integrals [1, 4], and other methods in [7, 25, 29, 33, 41] to solve the general NLEVP. In [5, 7] a very promising new method for PEPs is suggested that computes full invariant pairs, but in Jacobi–Davidson or Newton-type methods, often only one eigenvalue/eigenvector pair is determined at a time, e.g., when the algorithms in [21, 24, 26, 33, 40, 42, 48, 49, 50] are applied to solve the NLEVP. One way, then, to compute several successive eigenpairs is to deflate converged eigenvalue/eigenvectors from the NLEVP. In [15], an explicit nonequivalence low-rank deflation method is proposed for computing the smallest real eigenvalues of a special quadratic eigenvalue problem. Once the smallest positive eigenvalue is obtained, it is then transformed to zero by the deflation scheme, while all other eigenvalues remain unchanged. The next successive eigenvalue thus becomes the smallest positive eigenvalue of the transformed problem, which is then again solved by the proposed method. The concept of nonequivalence deflation is also applied to solve special quadratic problems in [20, 23] and cubic polynomial eigenvalue problems [22, 50]. One of the differences of the nonequivalence deflation scheme in [15] and

[20, 22, 23, 50] is that the convergent eigenvalue is transformed to infinity rather than 0.

Almost all currently available eigenvalue methods have major difficulties when multiple eigenvalues occur, because then the convergence of Newton-type methods deteriorates and in this case also the condition number of the problem typically is extremely large, so that small perturbations lead to large errors. In this case it is necessary to either consider block oriented methods [3, 5, 7, 36] which currently are designed for quadratic and polynomial problems or, in the more general nonlinear case, one needs to employ specially designed deflation techniques, such as the one we will discuss in this paper.

We consider large, sparse NLEVPs of the form

$$A\mathbf{x} = \omega(\omega B_n + \omega\varepsilon_d(\omega)B_d)\mathbf{x}, \tag{1.4}$$

arising from a 3D dispersive metallic PC with a face-centered cubic lattice, where A, B_n, B_d are large, sparse matrices, and the subscripts n and d indicate the nondispersive and the dispersive materials, respectively. This problem has a large number of zero eigenvalues, and the eigenvalues with smallest positive real part are of interest. Moreover, most of the desired eigenvalues are clustered so that it becomes an extremely challenging problem. To deal with this challenge, we propose a Newton-type iterative method with a special nonequivalence deflation scheme to solve (1.4).

By sequential application of the proposed nonequivalence deflation, we formulate the deflated NLEVPs as

$$A\tilde{\mathbf{x}} = \omega\widetilde{B}(\omega)\tilde{\mathbf{x}}, \tag{1.5}$$

where the desired eigenpairs are sequentially computed from a sequence of NLEVPs in (1.5). To solve (1.5), a novel Newton-type scheme is presented which solves in each step the generalized eigenvalue problem (GEP)

$$\beta A\tilde{\mathbf{x}} = \widetilde{B}(\omega_k)\tilde{\mathbf{x}}$$

starting from a sample frequency ω_k. We apply the nullspace-free method of [17, 19] and transform the GEP to a standard eigenvalue problem (SEP). Both the SEP and the GEP have the same nonzero finite eigenvalues. Furthermore, a heuristic strategy is proposed to determine the initial value ω_0 of the Newton-type method so that the desired eigenvalue clusters can be successfully computed. The quadratic convergence of the method is illustrated via numerical examples. The SEP can be solved by the Jacobi–Davidson method [43] or the shift-and-invert residual Arnoldi method [19, 30, 31]. An efficient FFT-based preconditioner is derived in the eigensolver so that the SEP can be efficiently solved. To make this method more practical, we discuss other strategies for determining initial vectors and stopping tolerances for the solution of the SEP, which reduce the computational cost and accelerate the convergence. Intensive numerical experiments show that our proposed method is robust and efficient to sequently compute the desired eigenpairs even though the desired eigenvalues are clustered.

This paper is organized as follows. In section 2, we briefly derive the NLEVP and the new nonequivalence low-rank deflation method. In section 3, we introduce the Newton-type method. The Jacobi–Davidson, the shift-invert residual Arnoldi, the nonlinear Arnoldi, and the nonlinear Jacobi-Davidson methods for solving the SEP and NLEVP, respectively, are reviewed in section 4. Some practical implementations to reduce the computational cost are proposed in section 5. Numerical experiments to validate the robustness of the proposed schemes are demonstrated in section 6. We conclude the paper in section 7.

2. Nonlinear eigenvalue problems.

In this section, we first introduce the resulting NLEVP by using the Yee scheme [51] for the discretization of the Maxwell equation (1.1). Then we propose a nonequivalence deflation scheme which allows us to transform the resulting NLEVP with eigenvalue/eigenvector pair $(\mu, \mathbf{x})$ to a new NLEVP with the same eigenvalues except that μ is replaced by infinity. Both the original and the deflated NLEVPs can be written in the form

$$A\mathbf{x} = \omega \widetilde{B}(\omega)\mathbf{x}. \tag{2.1}$$

In the next section, we will then develop a Newton-type method for solving (2.1) so that we can intertwine this method and the nonequivalence deflation scheme to compute the desired eigenvalue/eigenvector pairs.

Based on the Bloch theorem [28], we aim to find the Bloch eigenfunctions $E(\mathbf{r})$ for (1.1) satisfying the following quasi-periodicity condition:

$$E(\mathbf{r} + \mathbf{a}_\ell) = e^{\imath 2\pi \mathbf{k}\cdot \mathbf{a}_\ell} E(\mathbf{r})$$

for $\ell = 1, 2, 3$. Here, $2\pi\mathbf{k}$ is the Bloch wave vector in the first Brillouin zone [27] and the vectors $\mathbf{a}_\ell$ are the lattice translation vectors that span the primitive cell, which are extended periodically to form the dispersive metallic PC. In this paper, we focus on the face-centered cubic (FCC) lattice vectors, i.e.,

$$\mathbf{a}_1 = \frac{a}{\sqrt{2}}[1, 0, 0]^\top, \ \mathbf{a}_2 = \frac{a}{\sqrt{2}}\left[\frac{1}{2}, \frac{\sqrt{3}}{2}, 0\right]^\top, \ \mathbf{a}_3 = \frac{a}{\sqrt{2}}\left[\frac{1}{2}, \frac{1}{2\sqrt{3}}, \sqrt{\frac{2}{3}}\right]^\top$$

with lattice constant a.

Let n_1, n_2, and n_3 with $n = n_1 n_2 n_3$ be the number of grid points in the x, y, and z directions, respectively, and let δ_x, δ_y, and δ_z denote the associated grid lengths in the x, y, and z axial directions, respectively.

The resulting matrix A arising from the discretized double-curl operator using the Yee scheme [51] on a primitive cell is then of the form [16, 17, 18]

$$A = C^* C \in \mathbb{C}^{3n\times 3n}, \tag{2.2}$$

where

$$C = \begin{bmatrix} 0 & -C_3 & C_2 \\ C_3 & 0 & -C_1 \\ -C_2 & C_1 & 0 \end{bmatrix} \in \mathbb{C}^{3n\times 3n},$$

with

$$C_1 = I_{n_2 n_3} \otimes K_1 \in \mathbb{C}^{n\times n}, \ C_2 = I_{n_3} \otimes K_2 \in \mathbb{C}^{n\times n}, \ C_3 = K_3 \in \mathbb{C}^{n\times n}. \tag{2.3}$$

Here, $\otimes$ denotes the Kronecker product; see Appendix A.1 or [17] for the detailed definition of the pseudoperiodical matrices K_1, K_2, and K_3. The resulting NLEVP then has the form

$$F(\omega)\mathbf{x} \equiv \left(A - \omega^2 B(\omega)\right)\mathbf{x} = 0 \tag{2.4}$$

with

$$B(\omega) = B_n + \varepsilon_d(\omega) B_d, \tag{2.5}$$

where A is defined in (2.2), B_n, B_d are diagonal, and $\varepsilon_d(\omega)$ is the related permittivity of the dispersive material given in (1.2) and (1.3). The goal of the eigenvalue computation is to compute the eigenvalues of smallest positive real part and the associated eigenvectors.

To conduct the analysis of the NLEVP (2.4) we have the following definition and lemma.

Definition 2.1. *Let $F(\omega)$ be a rational matrix; i.e., all entries of $F(\omega)$ are rational in ω. Furthermore, suppose that $F(\omega)$ can be represented as*

$$F(\omega) = P(\omega) + R(\omega), \tag{2.6}$$

where $P(\omega)$ is a polynomial matrix of degree r and $R(\omega)$ is a rational matrix with entries being proper rational:

(a) *If $\omega_0 \in \mathbb{C}$ satisfies $\det(F(\omega_0)) = 0$, then ω_0 is an eigenvalue of $F(\omega)$. A nonzero vector $\mathbf{x}$ satisfying $F(\omega_0)\mathbf{x} = 0$ is then called the associated eigenvector corresponding to ω_0.*

(b) *$F(\omega)$ has an eigenvalue at infinity if $\lim_{\omega\to\infty} \det(\omega^{-r} F(\omega)) = 0$. A nonzero vector $\mathbf{x}$ satisfying $\lim_{\omega\to\infty}(\omega^{-r}F(\omega))\mathbf{x} = 0$ is then called the associated eigenvector corresponding to the infinite eigenvalue.*

Lemma 2.2. *Let $\varepsilon_d(\omega)$ be defined as in (1.2) or (1.3). Then $\overline{\varepsilon_d(\omega)} = \varepsilon_d(-\bar{\omega})$.*

Proof. From (1.2) and (1.3), we directly have

$$\overline{\varepsilon_d(\omega)} = 1 - \frac{\omega_p^2}{\bar{\omega}^2 - \imath\Gamma_p\bar{\omega}} = 1 - \frac{\omega_p^2}{(-\bar{\omega})^2 + \imath\Gamma_p(-\bar{\omega})} = \varepsilon_d(-\bar{\omega})$$

and

$$\begin{aligned}\overline{\varepsilon_d(\omega)} &= \varepsilon_\infty - \frac{\omega_p^2}{(\bar{\omega})^2 - \imath\Gamma_p\bar{\omega}} + \sum_{j=1}^{2} \Omega_j A_j \left(\frac{e^{-\imath\phi_j}}{\Omega_j - \bar{\omega} + \imath\Gamma_j} + \frac{e^{\imath\phi_j}}{\Omega_j + \bar{\omega} - \imath\Gamma_j} \right) \\ &= \varepsilon_d(-\bar{\omega}),\end{aligned}$$

respectively. □

With the help of Lemma 2.2 we have the following theorem.

Theorem 2.3. *The NLEVP (2.4) has the following properties:*

(a) *$F(\omega)$ has n zero eigenvalues and no eigenvalue at infinity.*

(b) *$F^*(\omega) = F(-\bar{\omega})$, i.e., ω and $-\bar{\omega}$ are eigenvalues of $F(\omega)$.*

(c) *If $\mathbf{y}$ is a left eigenvector of $F(\omega)$ corresponding to the eigenvalue ω, then $\mathbf{y}$ is a right eigenvector corresponding to the eigenvalue $-\bar{\omega}$.*

Proof. From (2.5) and the definition of $\varepsilon_d(\omega)$ in (1.2) or (1.3), it follows that $(\omega B(\omega))|_{\omega=0} = -\frac{\omega_p^2}{\imath\Gamma_p} B_d$. This implies that the eigenvectors of A corresponding to the zero eigenvalues are also the eigenvectors of $F(\omega)$ corresponding to the zero eigenvalues. Therefore, by Theorem 3.7 in [17], $F(\omega)$ has a semisimple zero eigenvalue with multiplicity n.

On the other hand, $F(\omega)$ can be represented as the form in (2.6) with degree r of $P(\omega)$ being equal to 2. Because $\lim_{\omega\to\infty} \omega^{-2}F(\omega)$ is equal to the nonsingular matrix

$B_n + B_d$ or $B_n + \varepsilon_\infty B_d$ for $\varepsilon_d(\omega)$ in (1.2) or (1.3), respectively, by the definition, $F(\omega)$ has no eigenvalue at infinity.

By the definition of $B(\omega)$ in (2.5) and Lemma 2.2, it follows that

$$\begin{aligned} F^*(\omega) &= A^* - (\bar{\omega})^2 \left(B_n + \overline{\varepsilon_d(\omega)} B_d \right) \\ &= A - (-\bar{\omega})^2 \left(B_n + \varepsilon_d(-\bar{\omega}) B_d \right) \\ &= F(-\bar{\omega}). \end{aligned}$$

This means that if $\mathbf{y}$ is the left eigenvector of $F(\omega)$ corresponding to ω, then

$$0 = F^*(\omega)\mathbf{y} = F(-\bar{\omega})\mathbf{y},$$

and, therefore, $\mathbf{y}$ is the right eigenvector corresponding to $-\bar{\omega}$. □

Let us assume that each of the pairwise different nonzero eigenvalues μ_j has equal algebraic and geometric multiplicity m_j, $j = 1, \ldots, \ell$, and let

$$X = \begin{bmatrix} X_1 & X_2 & \cdots & X_\ell \end{bmatrix} \tag{2.7}$$

with $X_j \in \mathbb{C}^{3n \times m_j}$, $j = 1, \ldots, \ell$, satisfy $X^* X = I_m$ with $m = m_1 + \cdots + m_\ell$. The following nonequivalence deflation allows us to transform the original problem (2.4) to a new NLEVP with the same eigenvalues, except that μ_i is replaced by infinity with multiplicity m_i for $i = 1, \ldots, \ell$. With

$$\widetilde{F}(\omega)\tilde{\mathbf{x}} := \left(F(\omega) \prod_{j=1}^{\ell} \left(I - \frac{\omega}{\omega - \mu_j} X_j X_j^* \right) \right) \tilde{\mathbf{x}}, \tag{2.8}$$

we have the following theorem.

THEOREM 2.4. *Let $F(\omega)$ and $\widetilde{F}(\omega)$ be defined as in* (2.4) *and* (2.8), *respectively. Then*

$$\begin{aligned} &\left\{ \omega | \ \widetilde{F}(\omega)\tilde{\mathbf{x}} = 0, \ \tilde{\mathbf{x}} \neq 0 \right\} \\ &\qquad = \ \{ \omega | \ F(\omega)\mathbf{x} = 0, \mathbf{x} \neq 0 \} \setminus \{ \mu_1, \ldots, \mu_1, \ldots, \mu_\ell, \ldots, \mu_\ell \} \cup \{ \infty \} . \end{aligned}$$

Furthermore, if $(\mu, \tilde{\mathbf{x}})$ is an eigenvalue/eigenvector pair of $\widetilde{F}(\omega)$, then $(\mu, \mathbf{x})$ is an eigenvalue/eigenvector pair of $F(\omega)$ with

$$\mathbf{x} = \prod_{j=1}^{\ell} \left(I - \frac{\mu}{\mu - \mu_j} X_j X_j^* \right) \tilde{\mathbf{x}}. \tag{2.9}$$

Proof. Since $X_i^* X_i = I_{m_i}$ for $i = 1, \ldots, \ell$, we have

$$(\lim_{\omega \to \infty} \omega^{-2} \widetilde{F}(\omega)) X_i = \left((B_n + \alpha B_d) \prod_{j=1}^{\ell} \left(I - X_j X_j^* \right) \right) X_i = 0,$$

where $\alpha = 1$ or $\alpha = \varepsilon_\infty$. This implies that $\widetilde{F}(\omega)$ has eigenvalue at infinity and the columns of X_i are the associated eigenvectors. Moreover, using the determinant identity $\det(I_n + RS) = \det(I_m + SR)$, where R and S^* are $n \times m$ matrices, we get

$$\begin{aligned}\det\left(\widetilde{F}(\omega)\right) &= \det\left(F(\omega)\right)\prod_{j=1}^{\ell}\det\left(I - \frac{\omega}{\omega-\mu_j}X_jX_j^*\right)\\ &= \det\left(F(\omega)\right)\prod_{j=1}^{\ell}\left(1-\frac{\omega}{\omega-\mu_j}\right)^{m_j}\\ &= \det\left(F(\omega)\right)\prod_{j=1}^{\ell}\left(\frac{-\mu_j}{\omega-\mu_j}\right)^{m_j}. \qquad (2.10)\end{aligned}$$

Because $\omega = \mu_j$ is a root with multiplicity m_j of $\det(F(\omega))$ by assumption, (2.10) implies that μ_j is *not* a root of $\det(\widetilde{F}(\omega))$. Hence, the nonlinear eigenvalue problem (2.8) has the same eigenvalues as (2.4), except that m_j copies of the eigenvalue μ_j are replaced by infinite eigenvalues.

From the definition of $\widetilde{F}(\omega)$ in (2.8), it is obvious to see that the vector $\mathbf{x}$ in (2.9) is an eigenvector of $F(\omega)$. □

Remark 1. In fact, in the nonequivalence deflation (2.8), the matrix X as in (2.7) can be a randomly constructed orthonormal matrix. However, the locking scheme used later in the nonlinear Arnoldi (NAr) algorithm needs to lock the convergent eigenvectors into the search subspace. So, we prefer to use the set of convergent eigenvectors to generate such a matrix X. If one of the convergent eigenvectors, $\mathbf{x}_i$, is linearly dependent on others, then we can randomly construct a vector to replace $\mathbf{x}_i$.

Using the fact that $X^*X = I_m$, we obtain

$$\prod_{j=1}^{\ell}\left(I - \frac{\omega}{\omega-\mu_j}X_jX_j^*\right) = I - \sum_{j=1}^{\ell}\frac{\omega}{\omega-\mu_j}X_jX_j^* = I - \omega X D(\omega) X^*, \qquad (2.11)$$

where

$$D(\omega) = \operatorname{diag}\left((\omega-\mu_1)^{-1}I_{m_1}, (\omega-\mu_2)^{-1}I_{m_2}, \ldots, (\omega-\mu_\ell)^{-1}I_{m_\ell}\right).$$

Plugging $F(\omega)$ of (2.4) and (2.11) into (2.8), $\widetilde{F}(\omega)$ can be reformulated in the following simple form:

$$\widetilde{F}(\omega) = A - \omega\left[\omega B(\omega) + (A - \omega^2 B(\omega))XD(\omega)X^*\right]. \qquad (2.12)$$

Define

$$\widetilde{B}(\omega) = \begin{cases} \omega B(\omega) & \text{for } F(\omega),\\ \omega B(\omega) + (A-\omega^2 B(\omega))XD(\omega)X^* & \text{for } \widetilde{F}(\omega).\end{cases} \qquad (2.13)$$

We then have that the NLEVPs (2.4) and (2.8) can both be represented in the form (2.1).

Note that, from the definition of $B(\omega)$ in (2.5) and Lemma 2.2, $B(\omega)$ is a complex diagonal matrix and $\omega B(\omega) + (A - \omega^2 B(\omega))XD(\omega)X^*$ is a complex diagonal plus a non-Hermitian low rank matrix.

Therefore, the desired eigenvalue/eigenvector pairs of $F(\omega)$, i.e., the ones with smallest positive real part, can be found by repeatedly solving deflated NLEVPs in (2.12) and using (2.9) in Theorem 2.4 to recover the eigenvector of $F(\omega)$. We summarize the computational process in Algorithm 1.

Algorithm 1. Nonequivalence deflated method for solving $A\mathbf{x} = \omega^2 B(\omega)\mathbf{x}$.

```
Input: Coefficient matrices $A$ (Hermitian) and $B(\omega)$.
Output: The desired eigenvalue/eigenvector pair $(\mu_d, \mathbf{x}_d)$ for $d = 1, \ldots, \ell$.
 1: Set $X = [\ ]$ and $\widetilde{B}(\omega) = \omega B(\omega)$.
 2: for $d = 1, \ldots, \ell$ do
 3:     Compute the desired eigenvalue/eigenvector pair $(\mu_d, \mathbf{x}_d)$ of $A\mathbf{x} = \omega \widetilde{B}(\omega)\mathbf{x}$;
 4:     % Retrieve the eigenvector of $Ax = \omega^2 B(\omega) x$ by Theorem 2.4
 5:     for $i = 1, \ldots, d-1$ do
 6:         Compute $\mathbf{x}_d = \left(I - \frac{\mu_d}{\mu_d - \mu_i}\tilde{\mathbf{x}}_i \tilde{\mathbf{x}}_i^*\right)\mathbf{x}_d$;
 7:     end for
 8:     % Compute the orthonormal matrix $X$ from the convergent
        eigenvectors
 9:     Set $\tilde{\mathbf{x}}_d = \mathbf{x}_d$; Orthogonalize $\tilde{\mathbf{x}}_d$ against $X$ and normalize $\tilde{\mathbf{x}}_d$;
10:     Expand $X = [X, \tilde{\mathbf{x}}_d]$;
11:     % Create the coefficient matrix of the new deflated nonlinear
        eigenvalue problem
12:     Set
            $\widetilde{B}(\omega) = \omega B(\omega) + (A - \omega^2 B(\omega)) X D(\omega) X^*,$
        where $D(\omega) = \operatorname{diag}\left((\omega - \mu_1)^{-1}, \ldots, (\omega - \mu_d)^{-1}\right)$;
13: end for
```

3. Newton-type methods.

Based on the Newton-type method suggested in [15], in this section, we will develop a Newton-type method for the computation of the desired eigenvalue/eigenvector pair for general NLEVPs of the form $A\mathbf{x} = \omega\widetilde{B}(\omega)\mathbf{x}$ in line 3 of Algorithm 1. In (2.1) for a given ω, we consider the GEP

$$\beta A\mathbf{x} = \widetilde{B}(\omega)\mathbf{x}, \tag{3.1}$$

where the eigenvalues β depend on the chosen value of ω. To determine an eigenvalue of (2.1), it is sufficient to find a value ω_* such that the eigenvalue $\beta(\omega_*)$ of (3.1) satisfies the condition $\beta(\omega_*) = \omega_*^{-1}$, which is equivalent to determining a root of the nonlinear equation

$$\beta(\omega) = \omega^{-1}. \tag{3.2}$$

The simplest method to solve this equation is to use a fixed-point iteration $\omega_{k+1} = \beta(\omega_k)^{-1}$, so that when it has converged to a value ω_*, then an eigenvalue $\beta(\omega_k)$ of (3.1) with $\omega = \omega_*$ has been computed. But the convergence of fixed-point iterations is typically linear. In this paper, we apply the Newton method

$$\omega_{k+1} = \omega_k - \left(\beta'(\omega_k) + \omega_k^{-2}\right)^{-1}\left(\beta(\omega_k) - \omega_k^{-1}\right) \tag{3.3}$$

to (3.2) to accelerate the convergence.

3.1. Nullspace-free method.

The success of Newton's method (3.3) is primarily based on reliable computation of $\beta(\omega_k)$ and $\beta'(\omega_k)$. However, such a reliable computation may not be guaranteed if one computes them directly using the original form of the eigenproblem $A\mathbf{x} = \omega\widetilde{B}(\omega)\mathbf{x}$, because the zero eigenvalue of multiplicity n severely interferes with our search for the eigenvalues of smallest positive real part.

To resolve this difficulty, we propose a nullspace-free method [17] that transforms the GEP (3.1) into an SEP of smaller dimension with the zero eigenvalue deflated. To this end, we present the following theorems and shall make use of them for computing $\beta'(\omega)$ reliably.

Theorem 3.1 (see [17]). *Let C_ℓ ($\ell = 1, 2, 3$) be as in* (2.3). *Then $C_i^* C_j = C_j C_i^*$, $C_i C_j = C_j C_i$, for $i, j = 1, 2, 3$, and all three matrices C_ℓ can be diagonalized by the same unitary matrix T, i.e.,*

$$C_1 T = T\Lambda_1,\ C_2 T = T\Lambda_2,\ \text{and } C_3 T = T\Lambda_3, \tag{3.4}$$

where Λ_1, Λ_2, and Λ_3 are diagonal matrices (see Appendix A.2 *for the definition of T).*

Theorem 3.2 (see [17]). *Let A and $(\Lambda_1, \Lambda_2, \Lambda_3, T)$ be defined as in* (2.2) *and* (3.4)*, respectively. Then there exists a unitary matrix*

$$\begin{bmatrix} Q_0 & Q \end{bmatrix} := (I_3 \otimes T) \begin{bmatrix} \Pi_0 & \Pi_1 \end{bmatrix} \equiv (I_3 \otimes T) \left[\begin{array}{c|cc} \Pi_{0,1} & \Pi_{1,1} & \Pi_{1,2} \\ \Pi_{0,2} & \Pi_{1,3} & \Pi_{1,4} \\ \Pi_{0,3} & \Pi_{1,5} & \Pi_{1,6} \end{array}\right],$$

where $\Pi_{0,i}$, $\Pi_{1,j} \in \mathbb{C}^{n\times n}$, $i = 1, 2, 3$, $j = 1, \dots, 6$, are diagonal and $\Pi_1 \in \mathbb{C}^{3n\times 2n}$ such that A has a unitary eigendecomposition in the form

$$\begin{bmatrix} Q_0 & Q \end{bmatrix}^* A \begin{bmatrix} Q_0 & Q \end{bmatrix} = \operatorname{diag}(0, \Lambda_q, \Lambda_q) \equiv \operatorname{diag}(0, \Lambda), \tag{3.5}$$

where $\Lambda_q = \Lambda_1^*\Lambda_1 + \Lambda_2^*\Lambda_2 + \Lambda_3^*\Lambda_3$.

In Theorem 3.2 it has been shown that with $n = n_1 n_2 n_3$ in the discretization (2.2) the matrix A has n zero eigenvalues. Because we are interested in finding the eigenvalues of (2.1) with smallest positive real parts, it means that the eigenvalues β^{-1} of the GEP $A\mathbf{x} = \beta^{-1}\widetilde{B}(\omega)\mathbf{x}$ with smallest positive real parts are of interest. In this respect, the large dimension of the invariant space corresponding to zero eigenvalues in the above GEP leads to several numerical difficulties; see [17]. To tackle this issue, the nullspace-free technique in Theorem 3.3 can be applied for solving (3.1) efficiently.

Theorem 3.3 (see [19]). *Let A be as in* (2.2)*, let (Q, Λ) be as in Theorem* 3.2*, and let ω satisfy $\widetilde{B}(\omega)$ in* (3.1) *being nonsingular. Then (denoting by span of a matrix the span of its columns)*

$$\operatorname{span}\widetilde{B}(\omega)^{-1}Q\Lambda^{1/2} = \operatorname{span}\left\{\mathbf{x} | A\mathbf{x} = \lambda\widetilde{B}(\omega)\mathbf{x},\ \lambda \neq 0\right\}$$

and, furthermore,

$$\left\{\lambda \neq 0 \,|\, A\mathbf{x} = \lambda\widetilde{B}(\omega)\mathbf{x}\right\} = \left\{\lambda \,|\, \Lambda^{1/2}Q^*\widetilde{B}(\omega)^{-1}Q\Lambda^{1/2}\mathbf{u} = \lambda\mathbf{u}\right\}.$$

Using Theorem 3.3, we can transform the $3n \times 3n$ GEP (3.1) to the $2n \times 2n$ SEP

$$K(\omega)^{-1}\mathbf{u} = \beta\mathbf{u}, \tag{3.6}$$

where

$$K(\omega) = \Lambda^{1/2}Q^*\widetilde{B}(\omega)^{-1}Q\Lambda^{1/2}, \tag{3.7}$$

and the GEP (3.1) and the SEP (3.6) have the same nonzero eigenvalues. The SEP can be solved by the eigensolver *without* being affected by zero eigenvalues.

3.2. Computing $\boldsymbol{\beta'(\omega)}$. To evaluate the derivative $\beta'(\omega)$ in (3.3) we can use the following method. Let $\mathbf{u}(\omega)$ and $\mathbf{v}(\omega)$ with $\mathbf{v}(\omega)^*\mathbf{u}(\omega) = 1$ be the right and the left eigenvectors of $K(\omega)^{-1}$, respectively, corresponding to the eigenvalue $\beta(\omega)$, i.e., $K(\omega)^{-1}\mathbf{u}(\omega) = \beta(\omega)\mathbf{u}(\omega)$ and $\mathbf{v}(\omega)^*K(\omega)^{-1} = \beta(\omega)\mathbf{v}(\omega)^*$. Then

$$\beta(\omega) = \mathbf{v}(\omega)^*K(\omega)^{-1}\mathbf{u}(\omega) \tag{3.8}$$

and

$$(\mathbf{v}(\omega)^*)'\mathbf{u}(\omega) + \mathbf{v}(\omega)^*\mathbf{u}(\omega)' = 0. \tag{3.9}$$

Using (3.8) and (3.9), and the fact that $(K(\omega)^{-1})' = -K(\omega)^{-1}K(\omega)'K(\omega)^{-1}$, we obtain

$$\begin{aligned}
\beta'(\omega) &= \mathbf{v}(\omega)^* \left(K(\omega)^{-1}\right)' \mathbf{u}(\omega) + (\mathbf{v}(\omega)^*)'K(\omega)^{-1}\mathbf{u}(\omega) + \mathbf{v}(\omega)^*K(\omega)^{-1}\mathbf{u}(\omega)' \\
&= -\mathbf{v}(\omega)^*K(\omega)^{-1}K(\omega)'K(\omega)^{-1}\mathbf{u}(\omega) + \beta(\omega)(\mathbf{v}(\omega)^*)'\mathbf{u}(\omega) + \beta(\omega)\mathbf{v}(\omega)^*\mathbf{u}(\omega)' \\
&= -\mathbf{v}(\omega)^*K(\omega)^{-1}K(\omega)'K(\omega)^{-1}\mathbf{u}(\omega) \\
&= -\beta(\omega)^2\mathbf{v}(\omega)^*K(\omega)'\mathbf{u}(\omega) \\
&= -\beta(\omega)^2\mathbf{v}(\omega)^*\Lambda^{1/2}Q^*\left[\widetilde{B}(\omega)^{-1}\right]'Q\Lambda^{1/2}\mathbf{u}(\omega) \\
&= \beta(\omega)^2\mathbf{v}(\omega)^*\Lambda^{1/2}Q^*\widetilde{B}(\omega)^{-1}\widetilde{B}(\omega)'\widetilde{B}(\omega)^{-1}Q\Lambda^{1/2}\mathbf{u}(\omega). \qquad (3.10)
\end{aligned}$$

```
**Algorithm 2.** Newton-type method for computing eigenvalues of $A\mathbf{x} = \omega\widetilde{B}(\omega)\mathbf{x}$.
**Input:** Coefficient matrices $A$ (Hermitian), $\widetilde{B}(\omega)$, an initial value $\omega_0$, and a stopping
    tolerance $tol$.
**Output:** An eigenvalue/eigenvector pair $(\mu_d, \mathbf{x}_d)$.
Set $k = 0$.
repeat
    Compute the eigenvalue $\beta_k^{-1}$ with the smallest positive real part and the asso-
    ciated eigenvector $\mathbf{u}_k$ of

    (3.11)    $\beta^{-1}\mathbf{u} = K(\omega_k)\mathbf{u} \equiv (\Lambda^{1/2}Q^*\widetilde{B}(\omega_k)^{-1}Q\Lambda^{1/2})\mathbf{u}$

    by the JD or SIRA method (see section 4 for details);
    Compute the left eigenvector $\mathbf{v}_k$ of (3.11) corresponding to $\beta_k$;
    Compute $\beta'(\omega_k)$ by

        $\beta'(\omega_k) = \beta_k^2\mathbf{v}_k^*\Lambda^{1/2}Q^*\widetilde{B}(\omega_k)^{-1}\widetilde{B}(\omega_k)'\widetilde{B}(\omega_k)^{-1}Q\Lambda^{1/2}\mathbf{u}_k;$

    Compute $\omega_{k+1}$ by

        $\omega_{k+1} = \omega_k - \left(\beta'(\omega_k) + \omega_k^{-2}\right)^{-1}\left(\beta_k - \omega_k^{-1}\right);$

    Set $k = k + 1$;
until $|\omega_k - \omega_{k-1}| < tol$.
Set $\mu_d = \omega_k$;
Compute the eigenvector $\mathbf{x}_d = \widetilde{B}(\omega_k)^{-1}Q\Lambda^{1/2}\mathbf{u}_k$.
```

We summarize the Newton-type method in Algorithm 2. For the calculation of $\beta'(\omega)$ in (3.10) and for solving SEP (3.6), it is required to compute $Q^*\tilde{\mathbf{p}}$, $Q\tilde{\mathbf{q}}$, and

$\widetilde{B}(\omega)^{-1}\mathbf{d}$ for given vectors $\tilde{\mathbf{p}}$, $\tilde{\mathbf{q}}$, and $\mathbf{d}$. For computing $Q^*\tilde{\mathbf{p}}$ and $Q\tilde{\mathbf{q}}$, the matrix Q itself does not need to be formed explicitly because the matrix-vector products $T^*\mathbf{p}$ and $T\mathbf{q}$ can be evaluated by the fast Fourier transform efficiently (see Algorithms 5 and 6 in Appendix A.2 for details). On the other hand, if $\widetilde{B}(\omega)$ is as in (2.12), then $\widetilde{B}(\omega)$ can be represented as

$$\widetilde{B}(\omega) = \omega B(\omega) + Y(\omega)X^*,$$

where

$$Y(\omega) = (A - \omega^2 B(\omega))XD(\omega).$$

Using the Sherman–Morrison–Woodbury formula [14] we get

$$\widetilde{B}(\omega)^{-1} = \omega^{-1}\left\{I - B(\omega)^{-1}Y(\omega)\left(\omega I + X^*B(\omega)^{-1}Y(\omega)\right)^{-1}X^*\right\}B(\omega)^{-1}. \tag{3.12}$$

By (3.12), to compute $\widetilde{B}(\omega)^{-1}\mathbf{d}$, it is necessary to evaluate $B(\omega)^{-1}\mathbf{d}$ and $B(\omega)^{-1}Y(\omega)$. Because $B(\omega)$ is diagonal and $Y(\omega)$ is low rank, $\widetilde{B}(\omega)^{-1}\mathbf{d}$ can be obtained at low cost.

3.3. Enhanced Newton-type method.

It is well known that the convergence of Newton's method is heavily dependent on the choice of the initial value. In particular, when the target roots of the nonlinear equation (3.2) are clustered, i.e., the NLEVP (2.4) has clustered eigenvalues, then the convergence is very sensitive to the choice of the initial value ω_0. Hence, it is very important to provide a good initial value to guarantee convergence. There are two problems in the choice of the initial value ω_0: (i) how to detect ω_0 which is good enough (i.e., for the case of well-separated eigenvalues); (ii) how to provide a new better initial value when ω_0 is not good enough (i.e., for the case of clustered eigenvalues).

In the kth Newton step, we need to solve the SEP (3.11). If the eigenvalue problem $A\mathbf{x} = \omega\widetilde{B}(\omega)\mathbf{x}$ has clustered eigenvalues which are of interest, then the convergence for solving (3.11) becomes very slow for a randomly chosen ω_0. Based on this observation, we propose in Algorithm 3 a heuristic strategy to tackle problems (i) and (ii) above. If the desired eigenvalue of (3.11) converges in a suitable iteration number m, it means that the provided initial value ω_0 is good enough. Otherwise, we switch to the approximate computation of a new approximate eigenpair $(\omega_0, \mathbf{x}_0)$ of NLEVP (2.4) by the nonlinear eigensolver, e.g., the nonlinear Arnoldi method (see the `if-endif` block in lines 5–10 of Algorithm 3), and resolve (3.11) with this new approximate eigenvalue ω_0. We repeat this process until $\{\omega_k\}$ converges (see the `while-endwhile` block in lines 3–11 of Algorithm 3).

After proposing the Newton-type method it remains to describe the eigenvalue solvers used in Algorithm 3. This is done in the next section.

4. Eigenvalue solvers.

In this section, we present eigenvalue algorithms for solving the SEP (3.11) in line 3 of Algorithm 2 and (3.13) in line 4 of Algorithm 3. Recall from section 3 that these SEPs are linearized and deflated variants of the original nonlinear eigenproblem $A\mathbf{x} = \omega\widetilde{B}(\omega)\mathbf{x}$. We shall also briefly discuss the nonlinear Arnoldi (NAr) method [48] and the nonlinear Jacobi–Davidson (NJD) method [49] as competitors for solving $A\mathbf{x} = \omega\widetilde{B}(\omega)\mathbf{x}$ directly.

4.1. Jacobi–Davidson method for the SEP (3.11).

The Jacobi–Davidson (JD) method [43] is an inexact eigenvalue solver for solving the SEP. In each iteration

Algorithm 3. Enhanced Newton-type method for computing smallest positive real part eigenvalues of $A\mathbf{x} = \omega\widetilde{B}(\omega)\mathbf{x}$.

```
Input: Coefficient matrices $A$ (Hermitian), $\widetilde{B}(\omega)$, initial value $\omega_0$, shift value $\sigma$, maximal iteration number $m$, the stopping tolerances $\tau_0$, $\tau_a$, and $tol$.
Output: The target eigenvalue/eigenvector pairs $(\mu_d, \mathbf{x}_d)$.
Set $k = 0$.
repeat
    while ( $\|\mathbf{r}_h\| \geq \tau_k$ ) do
        Compute the eigenvalue $\beta_k^{-1}$ with the smallest positive real part, the associated eigenvector $\mathbf{u}_k$ of
            (3.13)    $\beta^{-1}\mathbf{u} = (\Lambda^{1/2}Q^*\widetilde{B}(\omega_k)^{-1}Q\Lambda^{1/2})\mathbf{u}$,
        and the corresponding residual vector $\mathbf{r}_h$ by the JD or SIRA method with maximal iteration number $m$ and the stopping tolerance $\tau_k$;
        if ($\|\mathbf{r}_h\| \geq \tau_k$) then
            Use $\mathbf{u}_k$ to compute an approximate eigenvector $\mathbf{x}_0$ of NLEVP (2.4) (refer to (5.6)).
            Use the NAr method with initial vector $\mathbf{x}_0$ and suitable stopping tolerance $\tau_a$ to compute the approximate eigenvalue/eigenvector pair $(\omega_a, \mathbf{x}_a)$ of the NLEVP (2.4), where $\omega_a$ is the closest eigenvalue to $\sigma$.
            Use $\mathbf{x}_a$ to compute an approximate eigenvector $\mathbf{u}_0$ of (3.13) (refer to (5.8) and (5.9)).
            Set $\omega_k = \omega_a$.  % Use $(\omega_k, \mathbf{u}_0)$ as the new initial data to resolve $\beta^{-1}\mathbf{u} = K(\omega_k)\mathbf{u}$.
        end if
    end while
    Compute the left eigenvector $\mathbf{v}_k$ of (3.13) corresponding to $\beta_k$;
    Compute $\beta'(\omega_k)$ via
        $\beta'(\omega_k) = \beta_k^2\mathbf{v}_k^*\Lambda^{1/2}Q^*\widetilde{B}(\omega_k)^{-1}\widetilde{B}(\omega_k)'\widetilde{B}(\omega_k)^{-1}Q\Lambda^{1/2}\mathbf{u}_k$;
    Compute $\omega_{k+1}$ by
        $\omega_{k+1} = \omega_k - \left(\beta'(\omega_k) + \omega_k^{-2}\right)^{-1}\left(\beta_k - \omega_k^{-1}\right)$;
    Set $k = k + 1$ and determine stopping tolerance $\tau_k$;
until $|\omega_k - \omega_{k-1}| < tol$.
Set $\mu_d = \omega_k$ and compute the eigenvector $\mathbf{x}_d = \widetilde{B}(\omega_k)^{-1}Q\Lambda^{1/2}\mathbf{u}_k$.
```

of JD, the correction equation

$$(I - \mathbf{u}\mathbf{u}^*)\left(K(\omega_k) - \theta I\right)(I - \mathbf{u}\mathbf{u}^*)\,\mathbf{t} = -\mathbf{r}, \quad \mathbf{t}\perp\mathbf{u}, \tag{4.1}$$

is solved approximately by an iterative solver, where $K(\omega_k)$ is defined as in (3.11), $(\theta, \mathbf{u})$ is the Ritz pair of $K(\omega_k)$, and $\mathbf{r} = (K(\omega_k) - \theta I)\mathbf{u}$. Here, $\mathbf{t}\perp\mathbf{u}$ means that $\mathbf{t}$ is orthogonal to $\mathbf{u}$. In each iteration for solving (4.1) with a given ω_k, we need to solve a linear system of the form

$$M_p\mathbf{z} = \mathbf{d}, \quad \mathbf{z}\perp\mathbf{u}, \tag{4.2}$$

where $\mathbf{d}$ is a given vector and

$$M_p \equiv (I - \mathbf{u}\mathbf{u}^*)\, M_K\, (I - \mathbf{u}\mathbf{u}^*)\,,$$

with M_K being the preconditioner of $K(\omega_k) - \theta I$.

For the deflated NLEVP (2.8), one has from (3.7) and (3.12) that

$$K(\omega_k) - \theta I = \left(\Lambda^{1/2} Q^* (\omega_k^{-1} B(\omega_k)^{-1}) Q \Lambda^{1/2} - \theta I\right) - U(\omega_k)\Psi(\omega_k)^{-1} V(\omega_k)^*,$$

where

$$\begin{aligned} U(\omega_k) &= \omega_k^{-1} \Lambda^{1/2} Q^* B(\omega_k)^{-1} (A - \omega_k^2 B(\omega_k)) X, \\ V(\omega_k) &= \left[\omega_k^{-1} X^* B(\omega_k)^{-1} Q \Lambda^{1/2}\right]^*, \\ \Psi(\omega_k) &= D(\omega_k)^{-1} + \omega_k^{-1} X^* B(\omega_k)^{-1} (A - \omega_k^2 B(\omega_k)) X. \end{aligned}$$

Therefore, we take as preconditioner

$$\begin{aligned} M_K &= \left(\Lambda^{1/2} Q^* (\alpha_{a,k} I) Q \Lambda^{1/2} - \theta I\right) - U(\omega_k)\Psi(\omega_k)^{-1} V(\omega_k)^* \\ &:= \Omega_k - U(\omega_k)\Psi(\omega_k)^{-1} V(\omega_k)^*, \end{aligned} \tag{4.3}$$

where $\alpha_{a,k}$ is the arithmetic average of the diagonal elements of $\omega_k^{-1} B(\omega_k)^{-1}$ and

$$\Omega_k = \Lambda^{1/2} Q^* (\alpha_{a,k} I) Q \Lambda^{1/2} - \theta I = \alpha_{a,k} \Lambda - \theta I$$

is a complex diagonal matrix. By the Sherman–Morrison–Woodbury formula, we get

$$M_K^{-1} = \Omega_k^{-1} \left\{ I + U(\omega_k) \left(\Psi(\omega_k) - V(\omega_k)^* \Omega_k^{-1} U(\omega_k)\right)^{-1} V(\omega_k)^* \Omega_k^{-1} \right\} \tag{4.4}$$

and the linear system (4.2) can be easily solved via

$$\mathbf{z} = M_K^{-1}\mathbf{d} + \eta M_K^{-1}\mathbf{u} \quad \text{with} \quad \eta = -\frac{\mathbf{u}^* M_K^{-1}\mathbf{d}}{\mathbf{u}^* M_K^{-1}\mathbf{u}}.$$

4.2. Shift-invert residual Arnoldi method for the SEP (3.11).

The shift-invert residual Arnoldi (SIRA) method [19, 30, 31] is another inexact eigenvalue solver. In each iteration of SIRA, the linear residual system

$$(K(\omega_k) - \sigma I)\,\mathbf{t} = \mathbf{r} \tag{4.5}$$

is solved approximately by an iterative solver, where $\mathbf{r} = K(\omega_k)\mathbf{u} - \theta\mathbf{u}$ is the residual vector and σ is a fixed shift value. From (3.12), we have

$$\Lambda^{1/2} Q^* \widetilde{B}(\omega_k)^{-1} Q \Lambda^{1/2} = \omega_k^{-1} \Lambda^{1/2} Q^* B(\omega_k)^{-1} Q \Lambda^{1/2} - U(\omega_k)\Psi(\omega_k)^{-1} V(\omega_k)^*.$$

Using the construction of the preconditioner M_K in (4.3), we take

$$M_S = (\alpha_{a,k}\Lambda - \sigma I) - U(\omega_k)\Psi(\omega_k)^{-1} V(\omega_k)^*$$

as a preconditioner and rewrite the linear system (4.5) as

$$A_M \mathbf{t} = M_S^{-1}\mathbf{r}, \tag{4.6}$$

where

$$\begin{aligned} A_M &= M_S^{-1}\left[\Lambda^{1/2}Q^*\widetilde{B}(\omega_k)^{-1}Q\Lambda^{1/2} - \sigma I\right] \\ &= M_S^{-1}\left\{M_S + \Lambda^{1/2}Q^*\left[\omega^{-1}B(\omega_k)^{-1} - \alpha_{a,k}I\right]Q\Lambda^{1/2}\right\} \\ &= I + M_S^{-1}\Lambda^{1/2}Q^*\left[\omega_k^{-1}B(\omega_k)^{-1} - \alpha_{a,k}I\right]Q\Lambda^{1/2}. \end{aligned}$$

We summarize the JD and SIRA methods for solving the SEP (3.11) in Algorithm 4. Note that, in practice, a restart with search subspace contraction [16] is used in Algorithm 4.

Algorithm 4. JD/SIRA method for solving $K\mathbf{x} = \lambda\mathbf{x}$.

```
Input: matrix $K$, an initial matrix $\mathbb{V}_1$, real shift $\sigma$, tolerance $\tau$, and maximal number
    of iterations maxit. (A restarting scheme is used if it is needed.)
Output: The desired eigenvalue/eigenvector pair $(\lambda, \mathbf{x})$ of $K$ where $\lambda$ is closest to $\sigma$
    and the associated residual vector $\mathbf{r}$.
Set "solver" = "JD" or "SIRA."
Set $j = 1$ and $\mathbf{r}_0 = \mathbf{e}_1$.
repeat
  Compute $\mathbb{W}_j = K\mathbb{V}_j$ and $\mathbb{M}_j = \mathbb{V}_j^*\mathbb{W}_j$.
  while ( $j \le$ maxit and $\|\mathbf{r}_{j-1}\|_2 \ge \tau$ ) do
    Compute the eigenvalue/eigenvector pairs $(\theta_i, \mathbf{s}_i)$ of $\mathbb{M}_j\mathbf{s} = (\mathbb{V}_j^*K\mathbb{V}_j)s = \theta\mathbf{s}$
    with $\|\mathbf{s}_i\|_2 = 1$ and $|\theta_1 - \sigma| \le |\theta_2 - \sigma| \le \cdots$.
    Compute $\mathbf{u}_j = \mathbb{V}_j\mathbf{s}_1$ and $\mathbf{r}_j = (K - \theta_1 I)\mathbf{u}_j$.
    if ($\|\mathbf{r}_j\|_2 \ge \tau$) then
      if ("solver" = "SIRA") then
        Compute (approximate) solution $\mathbf{t}_j$ for
            $(K - \sigma I)\mathbf{t}_j = \mathbf{r}_j.$
      else if ("solver" = "JD") then
        Compute (approximate) solution $\mathbf{t}_j \perp \mathbf{u}_j$ for
            $\left(I - \mathbf{u}_j\mathbf{u}_j^*\right)(K - \theta_1 I)\left(I - \mathbf{u}_j\mathbf{u}_j^*\right)\mathbf{t}_j = -\mathbf{r}_j.$
      end if
      Orthogonalize $\mathbf{t}_j$ against $\mathbb{V}_j$; set $\mathbf{v}_{j+1} = \mathbf{t}_j/\|\mathbf{t}_j\|$.
      Compute $\mathbf{w}_{j+1} = K\mathbf{v}_{j+1}$, $\mathbb{M}_{j+1} = \begin{bmatrix} \mathbb{M}_j & \mathbb{V}_j^*\mathbf{w}_{j+1} \\ \mathbf{v}_{j+1}^*\mathbb{W}_j & \mathbf{v}_{j+1}^*\mathbf{w}_{j+1} \end{bmatrix}$.
      Expand $\mathbb{V}_{j+1} = [\mathbb{V}_j, \mathbf{v}_{j+1}]$ and $\mathbb{W}_{j+1} = [\mathbb{W}_j, \mathbf{w}_{j+1}]$.
    end if
    Set $j := j + 1$.
  end while
  if ($\|\mathbf{r}_{j-1}\|_2 \ge \tau$) then
    Set $\mathbb{V}_m = \mathbb{V}_{j-1}\begin{bmatrix} s_1 & \cdots & s_m \end{bmatrix}$, $\mathbf{r}_{m-1} = \mathbf{r}_{j-1}$, and $j = m$.
  end if
until desired eigenvalue/eigenvector is convergent
Set $\lambda = \theta_1$, $\mathbf{x} = \mathbf{u}_j$, $\mathbf{r} = \mathbf{r}_j$, and $\mathbb{V}_1 = \mathbb{V}_j[\mathbf{s}_1, \ldots, \mathbf{s}_p]$.
```

4.3. Nonlinear eigensolvers for the NLEVP (2.4). The NLEVP (2.4) can be solved by the NAr or NJD method directly. For a given search subspace V, let $(\tilde{\omega}, \tilde{\mathbf{z}})$ be an eigenvalue/eigenvector pair of the projected problem $V^*(A - \omega^2 B(\omega))V\mathbf{z} = 0$ and let $\tilde{\mathbf{x}} = V\tilde{\mathbf{z}}$ be the associated Ritz vector, i.e., the eigenvector lifted to the large space. The new search direction $\mathbf{v}$ in the NAr and NJD methods is chosen as

$$\mathbf{v} = \left(A - \sigma^2 B(\sigma)\right)^{-1} \mathbf{r} \tag{4.7}$$

and

$$\left(I - \frac{(2\tilde{\omega}B(\tilde{\omega}) + \tilde{\omega}^2 B(\tilde{\omega})')\tilde{\mathbf{x}}\tilde{\mathbf{x}}^*}{\tilde{\mathbf{x}}^*(2\tilde{\omega}B(\tilde{\omega}) + \tilde{\omega}^2 B(\tilde{\omega})')\tilde{\mathbf{x}}}\right)(A - \tilde{\omega}^2 B(\tilde{\omega}))\left(I - \frac{\tilde{\mathbf{x}}\tilde{\mathbf{x}}^*}{\tilde{\mathbf{x}}^*\tilde{\mathbf{x}}}\right)\mathbf{v} = -\mathbf{r}, \quad \mathbf{v}\perp\tilde{\mathbf{x}}, \tag{4.8}$$

respectively, where $\mathbf{r} = (A - \tilde{\omega}^2 B(\tilde{\omega}))\tilde{\mathbf{x}}$ is the residual vector for $(\tilde{\omega}, \tilde{\mathbf{x}})$ and σ is a given shift value. After reorthogonalizing $\mathbf{v}$ against V, the vector is appended to V and one repeats this process until $(\tilde{\omega}, \tilde{\mathbf{x}})$ converges to the desired eigenvalue/eigenvector pair.

The major cost of the NAr (NJD) method arises in solving (4.7) ((4.8)). This cost can be significantly reduced by using a technique suggested in [19]. Since $B(\sigma)$ in (2.4) is diagonal, we employ a preconditioner

$$M = A - \sigma^2 \alpha_\sigma I$$

and

$$M_J = \left(I - \frac{(2\tilde{\omega}B(\tilde{\omega}) + \tilde{\omega}^2 B(\tilde{\omega})')\tilde{\mathbf{x}}\tilde{\mathbf{x}}^*}{\tilde{\mathbf{x}}^*(2\tilde{\omega}B(\tilde{\omega}) + \tilde{\omega}^2 B(\tilde{\omega})')\tilde{\mathbf{x}}}\right)(A - \tilde{\omega}^2 \alpha_\sigma I)\left(I - \frac{\tilde{\mathbf{x}}\tilde{\mathbf{x}}^*}{\tilde{\mathbf{x}}^*\tilde{\mathbf{x}}}\right)$$

for solving (4.7) and (4.8), respectively, where α_σ is the arithmetic average of the diagonal elements of $B(\sigma)$. The associated linear system with coefficient matrix $(A - \gamma I)$ can be efficiently solved by applying the spectral decompositions of the matrices C_ℓ, $\ell = 1, 2, 3$; see [19] or Appendix A.3. Furthermore, we can apply the left-preconditioning M^{-1} to (4.7) and obtain the system

$$\left[I + \sigma^2 M^{-1}\left(\alpha_\sigma I - B(\sigma)\right)\right]\mathbf{v} = M^{-1}\mathbf{r},$$

which only requires computing $\mathbf{d} + \sigma^2 M^{-1}\left(\alpha_\sigma I - B(\sigma)\right)\mathbf{d}$ in each iteration for a given vector $\mathbf{d}$. There is no need to compute a matrix-vector multiplication with A.

5. Practical implementation. Suppose that we want to find ℓ smallest positive real part eigenvalues $\mu_1, \ldots, \mu_\ell$ of the NLEVP (2.4). In previous sections, we proposed a Newton-type method with nonequivalence deflation to sequentially compute the desired eigenvalues μ_d, $d = 1, \ldots, \ell$. Now, we briefly summarize it to further clarify the relation among the proposed algorithms for the computation of the dth eigenvalue/eigenvector of (2.4).

In Algorithm 1, sequentially applying the nonequivalence deflation, we formulate the deflated eigenvalue problems as

$$A\mathbf{x} = \omega\widetilde{B}(\omega)\mathbf{x}, \tag{5.1}$$

which is of the same form as the original eigenvalue problem. The Newton-type method in Algorithm 2 is then applied to solve (5.1) by successively solving the GEP

$$\beta A\mathbf{x} = \widetilde{B}(\omega_k^{(d)})\mathbf{x} \;\text{ for } k = 0, 1, 2, \ldots. \tag{5.2}$$

Each $3n \times 3n$ GEP in (5.2) is reduced into an $2n \times 2n$ SEP

$$\mathbf{u} = \beta \left(\Lambda^{1/2} Q^* \widetilde{B}(\omega_k^{(d)})^{-1} Q \Lambda^{1/2} \right) \mathbf{u} \tag{5.3}$$

by deflating out all zero eigenvalues of A. When the desired eigenvalues of (5.1) are clustered, we apply an enhanced Newton-type method in Algorithm 3 by using the NAr method for finding a good initial guess. The sequence of SEPs is then solved by JD or SIRA in Algorithm 4.

In the above, we develop a sequence of algorithms (Algorithms 1–4) for solving the NLEVP (2.4). In this section, we focus on the practical implementations including (i) the setting of the initial values and vectors, and (ii) the stopping tolerance of the associated solvers. These practical issues can significantly improve the efficiency and robustness of our proposed methods.

5.1. Initial value $\boldsymbol{\omega_0}$ and initial vector for Algorithms 2 and 4. As above, for finding the dth eigenpair in line 3 of Algorithm 1, a sequence of SEPs (5.3) arising from line 3 of Algorithm 2 or line 4 of Algorithm 3 is solved by Algorithm 4. In solving (5.3) with a given $\omega_k^{(d)}$, usually more than one Ritz pair is chosen at each jth iteration. Suppose that $(\beta_{1,j}^{(d)}, \mathbf{u}_{1,j}^{(d)})$, …, $(\beta_{m_1,j}^{(d)}, \mathbf{u}_{m_1,j}^{(d)})$ with $|(\beta_{1,j}^{(d)})^{-1} - \sigma| \leq \cdots \leq |(\beta_{m_1,j}^{(d)})^{-1} - \sigma|$ in line 6 of Algorithm 4 are chosen. When $\{\beta_{1,j}^{(d)}\}$ is converging to the desired eigenvalue of SEP (5.3) at the j_kth iteration, $\beta_{1,j_k}^{(d)}$ is applied to compute the next $\omega_{k+1}^{(d)}$, and the subspace $\operatorname{span}\{\mathbf{u}_{1,j_k}^{(d)}, \ldots, \mathbf{u}_{m_1,j_k}^{(d)}\}$ is used as the initial subspace $\mathbb{V}_1$ in Algorithm 4 for solving (5.3) with new $\omega_{k+1}^{(d)}$.

After d steps in Algorithm 1, the d eigenvalues/eigenvectors $(\mu_i, \mathbf{x}_i)$ for $i = 1, \ldots, d$ of the original problem $A\mathbf{x} = \omega^2 B(\omega)\mathbf{x}$ have been computed, and we now start the $(d+1)$st step in Algorithm 1, invoking Algorithm 2 for solving the new deflated NLEVP

$$\widetilde{F}(\omega)\tilde{\mathbf{x}} = F(\omega) \prod_{i=1}^{d} \left(I - \frac{\omega}{\omega - \mu_i} \tilde{\mathbf{x}}_i \tilde{\mathbf{x}}_i^* \right) \tilde{\mathbf{x}}, \tag{5.4}$$

where $\{\tilde{\mathbf{x}}_1, \ldots, \tilde{\mathbf{x}}_d\}$ is an orthonormal basis for the subspace $\operatorname{span}\{\mathbf{x}_1, \ldots, \mathbf{x}_d\}$. Applying the Newton-type method to solve (5.4), we need to give an initial value $\omega_0^{(d+1)}$. Here, we take $\omega_0^{(d+1)} = (\beta_{2,j_{k_d}}^{(d)})^{-1}$, the Ritz value obtained in Algorithm 4 that is subsequent to the Ritz value $(\beta_{1,j_{k_d}}^{(d)})^{-1}$ that has just converged to $\omega_{k_d}^{(d)} \approx \mu_d$. For the given initial $\omega_0^{(d+1)}$, it needs to solve the SEP

$$\mathbf{u} = \beta \left(\Lambda^{1/2} Q^* \widetilde{B}(\omega_0^{(d+1)})^{-1} Q \Lambda^{1/2} \right) \mathbf{u} \tag{5.5}$$

by Algorithm 4 with a given initial subspace. Now, we propose a method to construct the initial subspace from $\{\mathbf{u}_{2,j_{k_d}}^{(d)}, \ldots, \mathbf{u}_{m_1,j_{k_d}}^{(d)}\}$ as follows.

For convenience, we use $\mathbf{u}_{2,j_{k_d}}^{(d)}$ as an example. Because $\mathbf{u}_{2,j_{k_d}}^{(d)}$ is a Ritz vector of

$$\mathbf{u} = \beta \left(\Lambda^{1/2} Q^* \widetilde{B}(\omega_{k_d}^{(d)})^{-1} Q \Lambda^{1/2} \right) \mathbf{u},$$

from Theorem 3.3, we define

$$\hat{\mathbf{x}}_0^{(d+1)} \equiv \widetilde{B}(\omega_{k_d}^{(d)})^{-1} Q \Lambda^{1/2} \mathbf{u}_{2,j_{k_d}}^{(d)} = \widetilde{B}(\mu_d)^{-1} Q \Lambda^{1/2} \mathbf{u}_{2,j_{k_d}}^{(d)}$$

and use it to approximate the eigenvector of $A\mathbf{x} = \omega\widetilde{B}(\mu_d)\mathbf{x}$. From Theorem 2.4, we set

$$\mathbf{x}_0^{(d+1)} := \prod_{i=1}^{d-1}\left(I - \frac{\mu_d}{\mu_d - \mu_i}\tilde{\mathbf{x}}_i\tilde{\mathbf{x}}_i^*\right)\hat{\mathbf{x}}_0^{(d+1)} \tag{5.6}$$

and take the pair $(\omega_0^{(d+1)}, \mathbf{x}_0^{(d+1)})$ as an approximate eigenvalue/eigenvector pair of NLEVP (2.4). The associated residual vector $\mathbf{r}_2$ is equal to

$$\begin{aligned}\mathbf{r}_2 = F(\omega_0^{(d+1)})\mathbf{x}_0^{(d+1)} &= \widetilde{F}(\omega_0^{(d+1)})\prod_{i=1}^{d}\left(I - \frac{\omega_0^{(d+1)}}{\omega_0^{(d+1)} - \mu_i}\tilde{\mathbf{x}}_i\tilde{\mathbf{x}}_i^*\right)^{-1}\mathbf{x}_0^{(d+1)}\\ &:= \widetilde{F}(\omega_0^{(d+1)})\tilde{\mathbf{x}}_0^{(d+1)},\end{aligned} \tag{5.7}$$

where

$$\begin{aligned}\tilde{\mathbf{x}}_0^{(d+1)} &= \prod_{i=1}^{d}\left(I - \frac{\omega_0^{(d+1)}}{\omega_0^{(d+1)} - \mu_i}\tilde{\mathbf{x}}_i\tilde{\mathbf{x}}_i^*\right)^{-1}\mathbf{x}_0^{(d+1)} = \prod_{i=1}^{d}\left(I - \frac{\omega_0^{(d+1)}}{\mu_i}\tilde{\mathbf{x}}_i\tilde{\mathbf{x}}_i^*\right)\mathbf{x}_0^{(d+1)}\\ &= \mathbf{x}_0^{(d+1)} - \sum_{i=1}^{d}\frac{\omega_0^{(d+1)}}{\mu_i}\left(\tilde{\mathbf{x}}_i^*\mathbf{x}_0^{(d+1)}\right)\tilde{\mathbf{x}}_i.\end{aligned} \tag{5.8}$$

Therefore, we may take $(\omega_0^{(d+1)}, \tilde{\mathbf{x}}_0^{(d+1)})$ as an approximate eigenvalue/eigenvector pair for (5.4) and use

$$\mathbf{u}_0^{(d+1)} = \Lambda^{-1/2}Q^*\widetilde{B}(\omega_0^{(d+1)})\tilde{\mathbf{x}}_0^{(d+1)} \tag{5.9}$$

as an initial vector for solving (5.5). The numerical results in Figure 6.6 (see section 6) show that $\mathbf{u}_0^{(d+1)}$ is a good initial vector if $\omega_0^{(d+1)}$ is good enough.

5.2. Stopping tolerances. The sequence $\{\omega_k^{(d)}\}$ of index k is constructed by a sequence of eigenvalues of SEPs (5.3). In the Newton-type method, we need the accurate eigenvalue/eigenvector pair of (5.3) for each $\omega_k^{(d)}$. Actually, the concept of an inexact Newton method [44] can be applied to adaptively control the accuracy of the eigenvalue/eigenvector pairs to reduce the computational cost. This concept gives us that the closer $\omega_k^{(d)}$ is to μ_d, the more accurate the solution of (5.3) that is needed. Based on this concept, we propose a heuristic strategy for the construction of the stopping tolerance τ_k for $k > 0$, in solving (5.3) of Algorithm 3 with

$$\begin{aligned}\tau_k = \max\Bigg\{&\max\left\{5\cdot 10^{-12}, \frac{10^4\text{eps}}{2\sqrt{\delta_x^{-2} + \delta_y^{-2} + \delta_z^{-2}}}\right\},\\ &\min\left\{5\cdot 10^{-4}, 0.1\cdot|\omega_k^{(d)} - \omega_{k-1}^{(d)}|^2\right\}\Bigg\},\end{aligned} \tag{5.10}$$

where δ_x, δ_y, and δ_z denote the grid lengths in the x, y, and z axial directions, respectively. The stopping tolerance τ_0 for $\omega_0^{(d)}$ is set to be

$$\tau_0 = \begin{cases} 10^{-3} & \text{for } d = 1,\\ \min(10^{-3}, 0.1\cdot\|\mathbf{r}_2\|_2) & \text{for } d > 1,\end{cases} \tag{5.11}$$

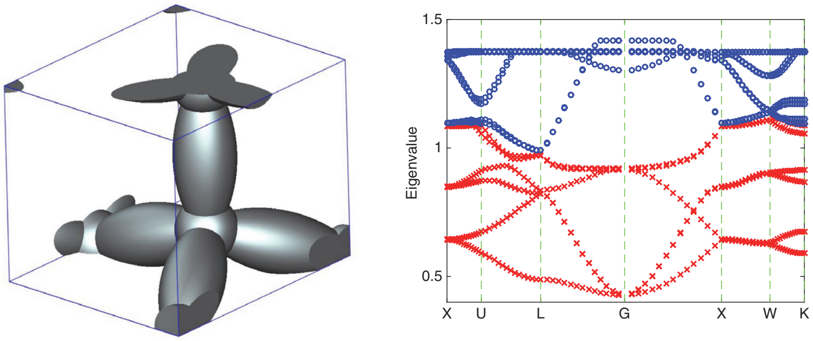

(a) Schema (b) Band structure diagram

FIG. 5.1. (a) *A schematic view of a dispersive metallic PC structure with an FCC lattice within a single primitive cell.* (b) *The computed band structure diagram of the Drude model with matrix dimension* $3 \cdot 48^3 = 331,776$. *There are* 16 *eigenvalues in the diagram. The six smallest real part nonzero eigenvalues* $\mu_1, \ldots, \mu_6$ *are denoted by (red)* ×.

where $\mathbf{r}_2$ is the residual vector in (5.7).

If a maximal number of JD/SIRA iterations is achieved but the Ritz vector does not converge, then NAr is applied to obtain a better initial data. In order to get useful initial data, we determine the stopping tolerance of NAr according to the concept that the closer we are to the eigenvalue/eigenvector pair of (5.3) for the Ritz value/vector pair by JD/SIRA, the smaller the stopping tolerance for NAr that is needed. According to this concept, the stopping tolerance of the residual norm for NAr at line 7 in Algorithm 3 is taken as

$$\tau_a = \max\left\{\min\left\{\|\mathbf{r}_h\|, 10^{-3}\right\}, 5 \times 10^{-8}\right\}, \tag{5.12}$$

where $\mathbf{r}_h$ is the residual vector of the approximate eigenvalue/eigenvector of (5.3) at line 4 in Algorithm 3. The stopping tolerance for solving the linear system (4.7) in NAr is set to be 10^{-4}. The heuristic strategies in [16] are applied to determine the maximal iteration number for solving the correction equation in JD and NJD. The associated stopping tolerance for solving the correction equation is set to 10^{-3}. As the results in [19] suggested, we set the stopping tolerance as 5×10^{-4} for (4.5) in SIRA.

6. Numerical results.

To study the numerical performance of the described methods for solving (2.4) arising in the 3D dispersive metallic PCs, we consider the setup described in [6, 17, 18]. The lattice in Figure 5.1(a) consists of spheres with a connecting spheroid. The radius r of the spheres is $r = 0.08a$, and the connecting spheroid has a minor axis length $s = 0.06a$ with $a = 2\pi$. The perimeter of the irreducible Brillouin zone for the lattice is formed by the corners $X = \frac{2\pi}{a}\Omega[0,1,0]^\top$, $U = \frac{2\pi}{a}\Omega\left[\frac{1}{4},1,\frac{1}{4}\right]^\top$, $L = \frac{2\pi}{a}\Omega\left[\frac{1}{2},\frac{1}{2},\frac{1}{2}\right]^\top$, $G = [0,0,0]^\top$, $W = \frac{2\pi}{a}\Omega\left[\frac{1}{2},1,0\right]^\top$, and $K = \frac{2\pi}{a}\Omega\left[\frac{3}{4},\frac{3}{4},0\right]^\top$, where

$$\Omega = \frac{1}{\sqrt{2}}\begin{bmatrix} 1 & 1 & 0 \\ -\frac{1}{\sqrt{3}} & \frac{1}{\sqrt{3}} & \frac{2}{\sqrt{3}} \\ \frac{2}{\sqrt{6}} & -\frac{2}{\sqrt{6}} & \frac{2}{\sqrt{6}} \end{bmatrix}.$$

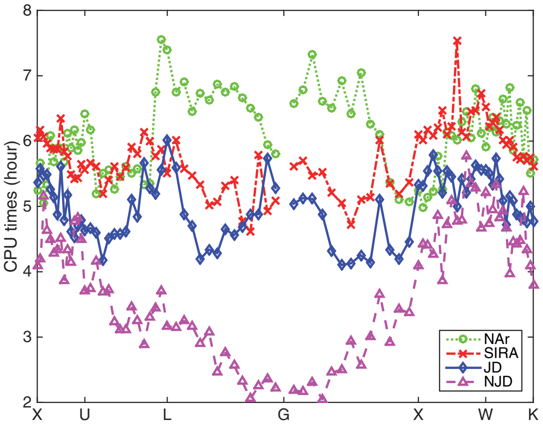

Fig. 6.1. *CPU times for computing the six smallest real part nonzero eigenvalues (and associated eigenvectors) denoted by (red)* × *in Figure* 5.1(b). *The matrix dimension is* 2, 654, 208.

The permittivity ε_n of the nondispersive material is set to be 1. Parameters in the Drude and Drude–Lorentz models are $\omega_p = \frac{10\pi}{a}$, $\Gamma_p = \frac{2\pi}{14500}$, $\Omega_1 = \frac{2\pi}{470}$, $\Omega_2 = \frac{2\pi}{325}$, $\Gamma_1 = \frac{2\pi}{1900}$, $\Gamma_2 = \frac{2\pi}{1060}$, $\varepsilon_\infty = 1.54$, $A_1 = 1.27$, $A_2 = 1.1$, $\phi_1 = -\frac{\pi}{4}$, and $\phi_2 = -\frac{\pi}{4}$ [34]. The associated band structure for the Drude model is shown in Figure 5.1(b). The band structure for the Drude–Lorentz model is similar to Figure 5.1(b).

All computations in this section are carried out in MATLAB 2013b, and some implementation details are addressed as follows. The MATLAB function `bicgstabl` is used to solve the linear systems in Algorithm 4, NJD, and NAr. On the other hand, the MATLAB functions `fft` and `ifft` are applied to compute the products $T^*\mathbf{p}$ and $T\mathbf{q}$, respectively.

For the hardware configuration, we use an HP DL360p Gen8 workstation that is equipped with two Intel Quad-Core Xeon E5-2643 3.33GHz CPUs, 96 GB of main memory, and the RedHat Enterprise Linux 6 operating system.

6.1. Comparison between Newton-type method and nonlinear eigensolvers. We demonstrate the efficiency of the new Newton-type method, NJD, and NAr in computing the six smallest positive real part eigenvalues $\mu_1, \ldots, \mu_6$ of the Drude model (1.2). The maximal dimension of the search subspace V in NJD and NAr is set to 35. When the dimension of V is larger than 35, then we take three Ritz vectors with associated Ritz values that are closest to the shift value as an initial subspace and restart the iteration.

The real parts of $\mu_1, \ldots, \mu_6$ are denoted by (red) × in Figure 5.1(b). As shown in the figure, these eigenvalues are well-separated so that they can be computed by the Newton-type method without using NAr to get the initial data. The CPU times for computing these six eigenvalue/eigenvector pairs by

- JD: Algorithm 1 + Algorithm 2 with solving (5.3) by JD,
- SIRA: Algorithm 1 + Algorithm 2 with solving (5.3) by SIRA,
- NAr: NAr method with fixed shift value σ for solving (2.4), and
- NJD: nonlinear JD method for solving (2.4)

are depicted in Figure 6.1, which shows that NJD obviously outperforms JD, SIRA, and NAr. Except for NJD, JD is much better than SIRA and NAr. Note that, in

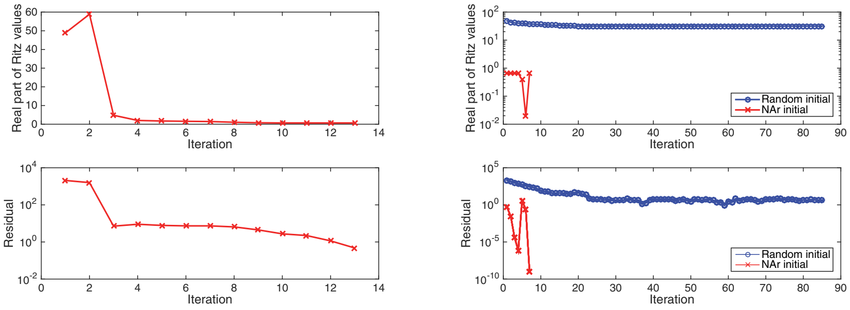

(a) Using NAr to compute an initial vector of NJD

(b) NJD with random initial vector and initial vector produced by NAr in Figure 6.2(a)

Fig. 6.2. *Convergence behavior of NJD using NAr for the initial vector and random initial vector, respectively, for computing the first desired eigenpair. The matrix dimension is* $2,654,208$.

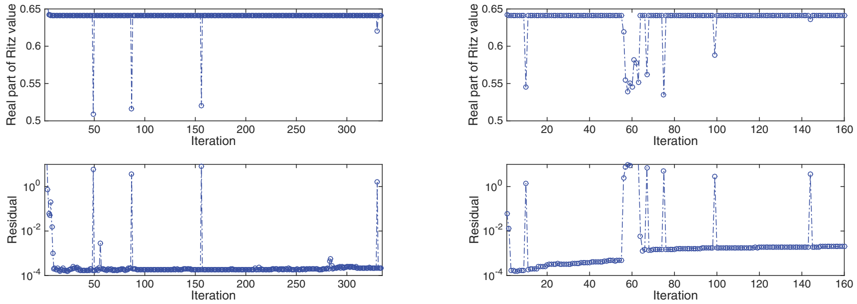

(a) NAr

(b) NJD

Fig. 6.3. *Convergence behavior of NAr and NJD for computing the first desired eigenpair* $\mu_1 \approx 0.6407596 - 2.377323 \times 10^{-4}\imath$ *of the Drude–Lorentz model at the wave vector* $\frac{4}{7}X + \frac{3}{7}W$. *The matrix dimension is* $2,654,208$.

practice, NAr is used to compute the initial vector of NJD for computing the first desired eigenvalue/eigenvector. If a random initial vector is used, then NJD would usually not converge for our benchmark problems, as shown in Figure 6.2.

The results in Figure 6.1 show that NAr and NJD can be successfully applied to compute the well-separated six eigenvalues of the Drude model (1.2). However, for the Drude–Lorentz model (1.3) whose nonlinearity is more complicated than the Drude model, Figure 6.3 shows that the Ritz values produced by NAr and NJD cannot converge to the first eigenvalue/eigenvector satisfying the stopping tolerance 10^{-10}.

Note that some of these Ritz values in Figure 6.3 are dragged toward 0.5 during the subspace iteration. This effect of dragging is also reflected in the convergence history of the residual. Figure 6.5 also shows the effect of dragging for the Ritz values. This effect is produced by the zero eigenvalue of multiplicity n. Due to this huge nullity, the Ritz vector associated with the Ritz value in Figure 6.3 or 6.5 easily contains the component of the null vectors. Such component results in dragging the Ritz value away from the desired eigenvalue, as shown in Figures 6.3 and 6.5.

6.2. Convergence of the Newton-type method. In this subsection, we illustrate the convergence of the Newton-type method in Algorithm 3 without using

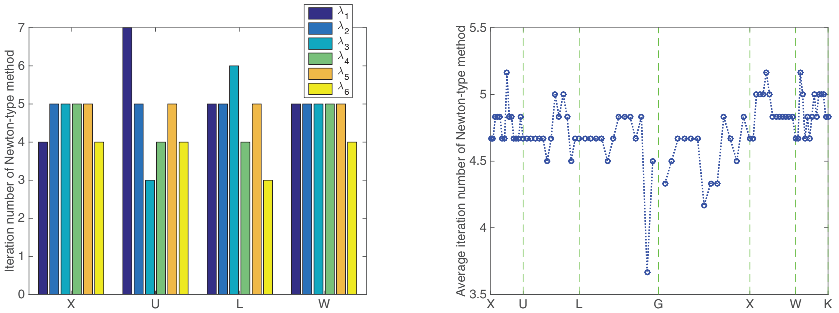

(a) Number of iterations k of the Newton-type method for computing each eigenvalue at wave vectors X, U, L, W, and K.

(b) Average number of iterations of the Newton-type method for computing six eigenvalues.

FIG. 6.4. *Number of iterations of Newton-type method with JD eigensolver for computing the six smallest real part nonzero eigenvalues denoted by (red) $\times$ in Figure* 5.1(b). *The matrix dimension is* $2,654,208$.

TABLE 6.1
Eigenvalues $\mu_7, \ldots, \mu_{14}$ *of* (2.4) *with the wave vector* $\frac{3}{7}X$ *and the matrix dimension* $2,654,208$.

	Drude model	Drude–Lorentz model
μ_7	$1.352760915 - 2.15717754 \times 10^{-4}\imath$	$1.326911260 - 2.11350594 \times 10^{-3}\imath$
μ_8	$1.352771023 - 2.15790978 \times 10^{-4}\imath$	$1.326915939 - 2.11375183 \times 10^{-3}\imath$
μ_9	$1.352771589 - 2.15790991 \times 10^{-4}\imath$	$1.326916471 - 2.11375357 \times 10^{-3}\imath$
μ_{10}	$1.352774278 - 2.15790186 \times 10^{-4}\imath$	$1.326919090 - 2.11375510 \times 10^{-3}\imath$
μ_{11}	$1.354710739 - 2.15785421 \times 10^{-4}\imath$	$1.328746727 - 2.11897302 \times 10^{-3}\imath$
μ_{12}	$1.354711852 - 2.15790561 \times 10^{-4}\imath$	$1.328747433 - 2.11899196 \times 10^{-3}\imath$
μ_{13}	$1.354711871 - 2.15790691 \times 10^{-4}\imath$	$1.328747439 - 2.11899260 \times 10^{-3}\imath$
μ_{14}	$1.354711899 - 2.15790684 \times 10^{-4}\imath$	$1.328747467 - 2.11899263 \times 10^{-3}\imath$

NAr for the estimation of the initial values of $\mu_1, \ldots, \mu_6$ discussed in the previous subsection. Using JD to solve the eigenvalue problem (3.11), the number of iterations k for computing each μ_i at wave vectors X, U, L, W, and K in the FCC lattice is depicted in Figure 6.4(a). We can see from this figure that only 3 to 7 iterations are needed for computing each eigenvalue. Figure 6.4(b) shows the average number of iterations for computing $\mu_1, \ldots, \mu_6$ with various wave vectors $\mathbf{k}$. The numerical experience indicates that the average ranges from 3.6 to 5.2 for all benchmark problems with the matrix dimension $3 \times 96^3 = 2,654,208$. This convergence behavior coincides with that of Newton's method for solving general nonlinear equations.

6.3. Clustered eigenvalues. From the band structure diagram in Figure 5.1(b) we see that the eigenvalues are clustered near 1.35 and 1.32 for the Drude and Drude–Lorentz models, respectively. Table 6.1 shows the clustering eigenvalues $\mu_7, \ldots, \mu_{14}$ of (2.4) (with the wave vector $\frac{3}{7}X$) of the Drude and Drude–Lorentz models, respectively. These clustering eigenvalues not only significantly increase the number of iterations for the NAr and lead to the nonconvergence of NJD, as shown in Figures 6.5, but also lead to a challenge for the Newton-type method: how to detect the clustering eigenvalues. In Figure 6.6, we depict the number of iterations of JD for computing eigenvalue/eigenvector pairs $(\beta_k, \mathbf{u}_k)$ of (3.11) in finding each $\mu_1, \ldots, \mu_7$ for the Drude model. For the specific wave vector U, $\mu_1, \ldots, \mu_7$ are well-separated. Figure 6.6(a)

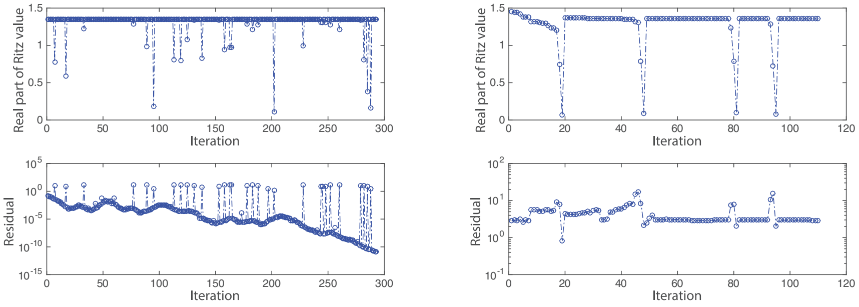

(a) NAr (b) NJD

FIG. 6.5. *Convergence behavior of the Ritz values (vs. number of iterations), produced by NAr and NJD, for computing μ_7 (at the wave vector $\frac{3}{7}X$) for the Drude model. The matrix dimension is* $2,654,208$.

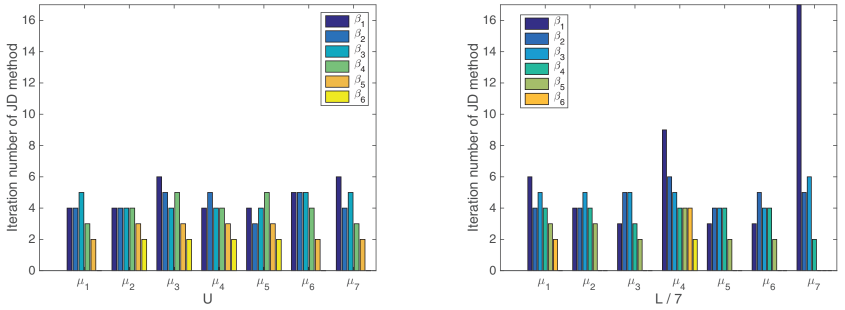

(a) $\mathbf{k} = U$ (b) $\mathbf{k} = \frac{1}{7}L$

FIG. 6.6. *Number of iterations of JD for computing eigenvalue β_k of* (3.11) *in Algorithm* 3 *at the wave vector* $\mathbf{k}$. *The matrix dimension is* $2,654,208$.

shows that all numbers of iterations of the JD method are less than 7. However, for wave vector $\frac{1}{7}L$, μ_7 is close to the clustering eigenvalues. The results in Figure 6.6(b) indicate that the number of iterations for computing β_1 in μ_7 is 17, which is obviously larger than that for other eigenvalues. This means that the number of iterations of the JD method are a crucial indicator for detecting clustering eigenvalues. In this example, we set the maximal number m of iterations to be 15 in Algorithm 3, and if JD is not convergent within 15 iterations, then the eigenvalues are regarded to be clustering and NAr is used to provide good initial data.

6.4. Efficiency of Algorithm 1 combined with Algorithm 3. Combining Algorithm 1 with the enhanced Newton-type method in Algorithm 3 with $m = 15$, the band structure diagram can be produced as in Figure 5.1(b). We consider six different wave vectors $\frac{4}{7}X + \frac{3}{7}U$, $\frac{4}{7}U + \frac{3}{7}L$, $\frac{4}{7}L$, $\frac{3}{7}X$, $\frac{4}{7}X + \frac{3}{7}W$, and $\frac{4}{7}W + \frac{3}{7}K$, and we take $n_1 = n_2 = n_3 = 96$; i.e., the matrix dimension is $2,654,208$. For each wave vector, 16 eigenvalues $\mu_1, \ldots, \mu_{16}$ are computed. For each eigenvalue μ_i, we depict the associated number of iterations k_i of the Newton-type method and the number of iterations p_i using NAr to get the initial data. The values of (k_i, p_i) for the Drude and the Drude–Lorentz models are shown in Figures 6.7(a)–(b) and 6.7(c)–(d),

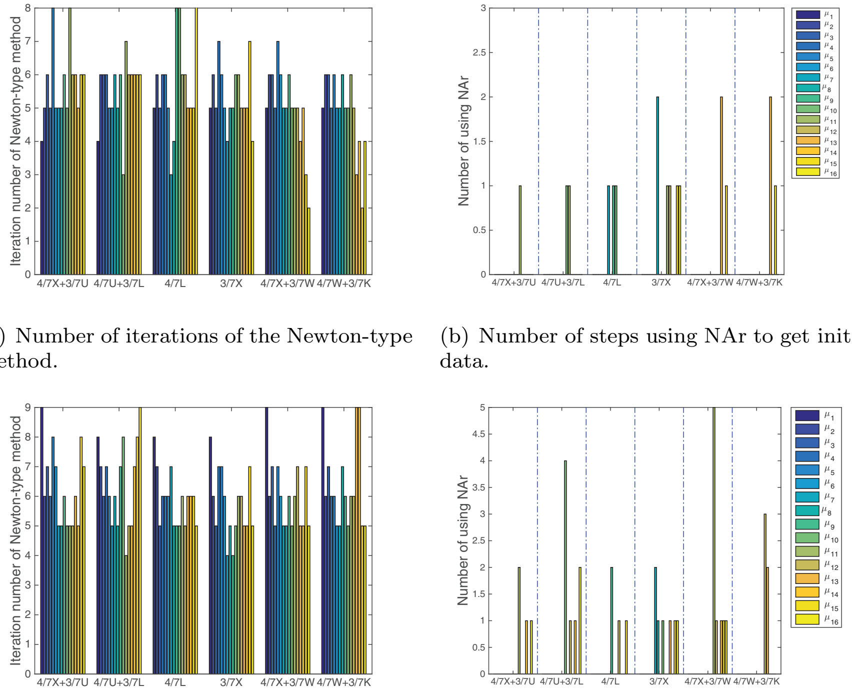

(a) Number of iterations of the Newton-type method.

(b) Number of steps using NAr to get initial data.

(c) Number of iterations of the Newton-type method.

(d) Number of steps using NAr to get initial data.

FIG. 6.7. *Number of iterations of the Newton-type method for computing eigenvalues* $\mu_1, \ldots,$ μ_{16}*, and number of steps of the NAr method for computing the initial value and vector for each eigenvalue/eigenvector pair at wave vectors* $\frac{4}{7}X + \frac{3}{7}U$, $\frac{4}{7}U + \frac{3}{7}L$, $\frac{4}{7}L$, $\frac{3}{7}X$, $\frac{4}{7}X + \frac{3}{7}W$, *and* $\frac{4}{7}W + \frac{3}{7}K$*. The matrix dimension is* $3 \times 96^3 = 2,654,208$. (a) *and* (b) *are the results for the Drude model;* (c) *and* (d) *are the results for the Drude–Lorentz model.*

respectively. In our proposed method, we not only use NAr to provide an initial datum for the eigenvalue/eigenvector pair, but we also use the strategies in subsection 5.1 to confirm convergence. Therefore, even if the eigenvalues are strongly clustered, as shown in Table 6.1, we can still compute the desired eigenvalue/eigenvector pairs within a reasonable (k_i, p_i), as shown in Figure 6.7.

7. Conclusions. Solving the nonlinear eigenvalue problem (NLEVP) arising from Yee's discretization of a 3D dispersive metallic PC is a computational challenge. We have proposed a Newton-type method to compute one desired eigenvalue/eigenvector pair of the NLEVP at a time. Once the desired eigenvalue is converged, it is then transformed to infinity by the proposed nonequivalence deflation scheme, while all other eigenvalues remain unchanged. The next successive eigenvalue thus becomes the smallest nonzero real part eigenvalue of the transformed NLEVP which is then again solved by the Newton-type method. Furthermore, some heuristic strategies for the determination of initial data and stopping tolerances of the iterative eigenvalue methods are introduced to accelerate the convergence. In order to compute the clustering eigenvalues of the NLEVP, we propose a hybrid method by using the JD or the SIRA method to solve the standard eigenvalue problems in the Newton-type method and NAr to compute the initial data. The numerical results demonstrate that our proposed method is robust and outperforms NAr and NJD for solving both the well-separated and the clustering eigenvalues of the NLEVP for the Drude–Lorentz model.

Appendix.

A.1. The matrices K_i, $i = 1, 2, 3$, in (2.3) are defined as

$$K_1 = \frac{1}{\delta_x} \begin{bmatrix} -1 & 1 & & \\ & \ddots & \ddots & \\ & & -1 & 1 \\ e^{\imath 2\pi \mathbf{k}\cdot\mathbf{a}_1} & & & -1 \end{bmatrix} \in \mathbb{C}^{n_1 \times n_1},$$

$$K_2 = \frac{1}{\delta_y} \begin{bmatrix} -I_{n_1} & I_{n_1} & & \\ & \ddots & \ddots & \\ & & -I_{n_1} & I_{n_1} \\ e^{\imath 2\pi \mathbf{k}\cdot\mathbf{a}_2} J_2 & & & -I_{n_1} \end{bmatrix} \in \mathbb{C}^{(n_1 n_2)\times(n_1 n_2)},$$

$$K_3 = \frac{1}{\delta_z} \begin{bmatrix} -I_{n_1 n_2} & I_{n_1 n_2} & & \\ & \ddots & \ddots & \\ & & -I_{n_1 n_2} & I_{n_1 n_2} \\ e^{\imath 2\pi \mathbf{k}\cdot\mathbf{a}_3} J_3 & & & -I_{n_1 n_2} \end{bmatrix} \in \mathbb{C}^{n \times n},$$

with

$$J_2 = \begin{bmatrix} 0 & e^{-\imath 2\pi \mathbf{k}\cdot\mathbf{a}_1} I_{n_1/2} \\ I_{n_1/2} & 0 \end{bmatrix} \in \mathbb{C}^{n_1 \times n_1},$$

$$J_3 = \begin{bmatrix} 0 & e^{-\imath 2\pi \mathbf{k}\cdot\mathbf{a}_2} I_{\frac{1}{3}n_2} \otimes I_{n_1} \\ I_{\frac{2}{3}n_2} \otimes J_2 & 0 \end{bmatrix} \in \mathbb{C}^{(n_1 n_2)\times(n_1 n_2)}.$$

A.2. Unitary matrix T in (3.4) is defined as

$$T = \frac{1}{\sqrt{n_1 n_2 n_3}} \begin{bmatrix} T_1 & T_2 & \cdots & T_{n_1} \end{bmatrix} \in \mathbb{C}^{n \times n}$$

with $T_i = \begin{bmatrix} T_{i,1} & T_{i,2} & \cdots & T_{i,n_2} \end{bmatrix} \in \mathbb{C}^{n \times (n_2 n_3)}$ and

$$T_{i,j} = \begin{bmatrix} \mathbf{z}_{i,j,1} \otimes \mathbf{y}_{i,j} \otimes \mathbf{x}_i & \mathbf{z}_{i,j,2} \otimes \mathbf{y}_{i,j} \otimes \mathbf{x}_i & \cdots & \mathbf{z}_{i,j,n_3} \otimes \mathbf{y}_{i,j} \otimes \mathbf{x}_i \end{bmatrix} \in \mathbb{C}^{n \times n_3}$$

for $i = 1, \ldots, n_1$, $j = 1, \ldots, n_2$, and $k = 1, \ldots, n_3$, where

$$\begin{aligned} \mathbf{x}_i &= E_{\mathbf{x}} \begin{bmatrix} 1 & e^{\theta_{\mathbf{x},i}} & \cdots & e^{(n_1-1)\theta_{\mathbf{x},i}} \end{bmatrix}^\top \equiv E_{\mathbf{x}} \mathbf{u}_{\mathbf{x},i}, \\ \mathbf{y}_{i,j} &= E_{\mathbf{y},i} \begin{bmatrix} 1 & e^{\theta_{\mathbf{y},j}} & \cdots & e^{(n_2-1)\theta_{\mathbf{y},j}} \end{bmatrix}^\top \equiv E_{\mathbf{y},i} \mathbf{u}_{\mathbf{y},j}, \\ \mathbf{z}_{i,j,k} &= E_{\mathbf{z},i+j} \begin{bmatrix} 1 & e^{\theta_{\mathbf{z},k}} & \cdots & e^{(n_3-1)\theta_{\mathbf{z},k}} \end{bmatrix}^\top \equiv E_{\mathbf{z},i+j} \mathbf{u}_{\mathbf{z},k} \end{aligned}$$

and

$$\begin{aligned}
\theta_i &= \frac{\imath 2\pi i}{n_1} + \frac{\imath 2\pi \mathbf{k}\cdot\mathbf{a}_1}{n_1} \equiv \theta_{\mathbf{x},i} + \varepsilon_{\mathbf{x}},\\
\theta_{i,j} &= \frac{\imath 2\pi j}{n_2} + \frac{\imath 2\pi}{n_2}\left\{\mathbf{k}\cdot\left(\mathbf{a}_2 - \frac{1}{2}\mathbf{a}_1\right) - \frac{i}{2}\right\} \equiv \theta_{\mathbf{y},j} + \varepsilon_{\mathbf{y},i},\\
\theta_{i,j,k} &= \frac{\imath 2\pi k}{n_3} + \frac{\imath 2\pi}{n_3}\left\{\mathbf{k}\cdot\left(\mathbf{a}_3 - \frac{1}{3}\left(\mathbf{a}_1 + \mathbf{a}_2\right)\right) - \frac{1}{3}(i+j)\right\} \equiv \theta_{\mathbf{z},k} + \varepsilon_{\mathbf{z},i+j}.
\end{aligned}$$

Here, $E_{\mathbf{x}} = \operatorname{diag}\left(1, e^{\varepsilon_{\mathbf{x}}}, \ldots, e^{(n_1-1)\varepsilon_{\mathbf{x}}}\right)$, $E_{\mathbf{y},i} = \operatorname{diag}\left(1, e^{\varepsilon_{\mathbf{y},i}}, \cdots, e^{(n_2-1)\varepsilon_{\mathbf{y},i}}\right)$, and $E_{\mathbf{z},i+j} = \operatorname{diag}\left(1, e^{\varepsilon_{\mathbf{z},i+j}}, \ldots, e^{(n_3-1)\varepsilon_{\mathbf{z},i+j}}\right)$. Denote

$$\begin{aligned}
U_{\mathbf{x}} &= \begin{bmatrix}\mathbf{u}_{\mathbf{x},1} & \mathbf{u}_{\mathbf{x},2} & \cdots & \mathbf{u}_{\mathbf{x},n_1}\end{bmatrix},\\
U_{\mathbf{y}} &= \begin{bmatrix}\mathbf{u}_{\mathbf{y},1} & \mathbf{u}_{\mathbf{y},2} & \cdots & \mathbf{u}_{\mathbf{y},n_2}\end{bmatrix},\\
U_{\mathbf{z}} &= \begin{bmatrix}\mathbf{u}_{\mathbf{z},1} & \mathbf{u}_{\mathbf{z},2} & \cdots & \mathbf{u}_{\mathbf{z},n_3}\end{bmatrix}.
\end{aligned}$$

Then the matrix-vector products of $T^*\mathbf{p}$ and $T\mathbf{q}$ can be efficiently computed by Algorithms 5 and 6, respectively.

Algorithm 5. Forward FFT-based matrix-vector product $T^*\mathbf{p}$ [17].

Input: Any vector $\mathbf{p} = \begin{bmatrix}\mathbf{p}_1^\top & \cdots & \mathbf{p}_{n_3}^\top\end{bmatrix}^\top \in \mathbb{C}^n$ with $\mathbf{p}_k = \begin{bmatrix}\mathbf{p}_{1,k}^\top & \cdots & \mathbf{p}_{n_2,k}^\top\end{bmatrix}^\top$ and $\mathbf{p}_{j,k} \in \mathbb{C}^{n_1}$ for $j = 1, \ldots, n_2$, $k = 1, \ldots, n_3$.

Output: The vector $\mathbf{f} \equiv T^*\mathbf{p}$.

```
for $k = 1, \ldots, n_3$ do
    Compute $P_{\mathbf{x}}(:,:,k) = \begin{bmatrix}\mathbf{p}_{1,k} & \cdots & \mathbf{p}_{n_2,k}\end{bmatrix}^* E_{\mathbf{x}} U_{\mathbf{x}}$.
end for
for $i = 1, \ldots, n_1$ do
    Compute $P_{\mathbf{y}} = \begin{bmatrix}P_{\mathbf{x}}(:,i,1) & P_{\mathbf{x}}(:,i,2) & \cdots & P_{\mathbf{x}}(:,i,n_3)\end{bmatrix}^\top E_{\mathbf{y},i} U_{\mathbf{y}}$.
    Compute $P_{\mathbf{z}} = U_{\mathbf{z}}^* \begin{bmatrix}E_{\mathbf{z},i+1}^* \bar{P}_{\mathbf{y}}(:,1) & E_{\mathbf{z},i+2}^* \bar{P}_{\mathbf{y}}(:,2) & \cdots & E_{\mathbf{z},i+n_2}^* \bar{P}_{\mathbf{y}}(:,n_2)\end{bmatrix}$.
    Set $\mathbf{f}((i-1)n_2 n_3 + 1 : i n_2 n_3) = \frac{1}{\sqrt{n_1 n_2 n_3}} \operatorname{vec}(P_{\mathbf{z}})$.
end for
```

Algorithm 6. Backward FFT-based matrix-vector product $T\mathbf{q}$ [17].

Input: Any vector $\mathbf{q} = \begin{bmatrix}\mathbf{q}_1^\top & \cdots & \mathbf{q}_{n_1}^\top\end{bmatrix}^\top \in \mathbb{C}^n$ with $\mathbf{q}_i = \begin{bmatrix}\mathbf{q}_{i,1}^\top & \cdots & \mathbf{q}_{i,n_2}^\top\end{bmatrix}^\top$ and $\mathbf{q}_{i,j} \in \mathbb{C}^{n_3}$ for $i = 1, \ldots, n_1$, $j = 1, \ldots, n_2$.

Output: The vector $\mathbf{g} \equiv T\mathbf{q}$.

```
for $i = 1, \ldots, n_1$ do
    Compute $Q_{\mathbf{z},i} = U_{\mathbf{z}} \begin{bmatrix}\mathbf{q}_{i,1} & \mathbf{q}_{i,2} & \cdots & \mathbf{q}_{i,n_2}\end{bmatrix}$.
    Update $Q_{\mathbf{z},i} := \begin{bmatrix}E_{\mathbf{z},i+1} Q_{\mathbf{z},i}(:,1) & E_{\mathbf{z},i+2} Q_{\mathbf{z},i}(:,2) & \cdots & E_{\mathbf{z},i+n_2} Q_{\mathbf{z},i}(:,n_2)\end{bmatrix}^\top$.
    Compute $Q_{\mathbf{y}}(:,:,i) = E_{\mathbf{y},i}\left(U_{\mathbf{y}} Q_{\mathbf{z},i}\right)$
end for
for $k = 1, \ldots, n_3$ do
    Compute $Q_{\mathbf{x}} = E_{\mathbf{x}} U_{\mathbf{x}} \begin{bmatrix}Q_{\mathbf{y}}(:,k,1) & Q_{\mathbf{y}}(:,k,2) & \cdots & Q_{\mathbf{y}}(:,k,n_1)\end{bmatrix}^\top$.
    Set $\mathbf{g}((k-1)n_1 n_2 + 1 : k n_1 n_2) = \frac{1}{\sqrt{n_1 n_2 n_3}} \operatorname{vec}(Q_{\mathbf{x}})$.
end for
```

A.3. Using Theorem 3.1, it holds that

$$A = I_3 \otimes (G^* G) - GG^*,$$

where $G = [C_1^\top, C_2^\top, C_3^\top]^\top$. Applying the eigendecompositions of C_ℓ's in Theorem 3.1 and the fact that $CG = 0$, the solution of the linear system

$$(A - \tau I)\mathbf{y} = \mathbf{d}$$

can be computed by

$$(I_3 \otimes \Lambda_q - \tau I)\,\tilde{\mathbf{y}} = \left(I - \tau^{-1} \begin{bmatrix} \Lambda_1 \\ \Lambda_2 \\ \Lambda_3 \end{bmatrix} \begin{bmatrix} \Lambda_1^* & \Lambda_2^* & \Lambda_3^* \end{bmatrix} \right) (I_3 \otimes T)^* \,\mathbf{d}$$

and

$$\mathbf{y} = (I_3 \otimes T)\,\tilde{\mathbf{y}}.$$

Acknowledgment. The authors thank the anonymous referees for their useful comments and suggestions.

REFERENCES

[1] J. Asakura, T. Sakurai, H. Tadano, T. Ikegami, and K. Kimura, *A numerical method for nonlinear eigenvalue problems using contour integrals*, JSIAM Lett., 1 (2009), pp. 52–55, doi:10.14495/jsiaml.1.52.

[2] Z. Bai, J. Demmel, J. Dongarra, A. Ruhe, and H. van der Vorst, *Templates for the Solution of Algebraic Eigenvalue Problems: A Practical Guide*, SIAM, Philadelphia, 2000, doi:10.1137/1.9780898719581.

[3] C. G. Baker, U. L. Hetmaniuk, R. B. Lehoucq, and H. K. Thornquis, *Anasazi software for the numerical solution of large-scale eigenvalue problems*, ACM Trans. Math. Software, 36 (2009), 13, doi:10.1145/1527286.1527287.

[4] W.-J. Beyn, *An integral method for solving nonlinear eigenvalue problems*, Linear Algebra Appl., 436 (2012), pp. 3839–3863, doi:10.1016/j.laa.2011.03.030.

[5] W.-J. Beyn, C. Effenberger, and D. Kressner, *Continuation of eigenvalues and invariant pairs for parameterized nonlinear eigenvalue problems*, Numer. Math., 119 (2011), pp. 489–516, doi:10.1007/s00211-011-0392-1.

[6] R.-L. Chern, C.-C. Chang, C.-C. Chang, and R.-R. Hwang, *Numerical study of three-dimensional photonic crystals with large band gaps*, J. Phys. Soc. Japan, 73 (2004), pp. 727–737, doi:10.1143/JPSJ.73.727.

[7] C. Effenberger, *Robust Solution Methods for Nonlinear Eigenvalue Problems*, Ph.D. thesis, Ecole polytechnique federale de Lausanne, Lausanne, Switzerland, 2013.

[8] C. Engström, C. Hafner, and K. Schmidt, *Computations of lossy Bloch waves in two-dimensional photonic crystals*, J. Comput. Theor. Nanosci., 6 (2009), pp. 1–9, doi:10.1166/jctn.2009.1108.

[9] C. Engström and M. Wang, *Complex dispersion relation calculations with the symmetric interior penalty method*, Internat. J. Numer. Methods Engrg., 84 (2010), pp. 849–863, doi:10.1002/nme.2926.

[10] P. G. Etchegoin, E. C. Le Ru, and M. Meyer, *An analytic model for the optical properties of gold*, J. Chem. Phys., 125 (2006), 164705, doi:10.1063/1.2360270.

[11] P. G. Etchegoin, E. C. Le Ru, and M. Meyer, *Erratum: "An analytic model for the optical properties of gold" [J. Chem. Phys.* 125, 164705 (2006)*]*, J. Chem. Phys., 127 (2007), 189901, doi:10.1063/1.2802403.

[12] S. Fan, P. R. Villeneuve, and J. D. Joannopoulos, *Large omnidirectional band gaps in metallodielectric photonic crystals*, Phys. Rev. B, 54 (1996), pp. 11245–11251, doi:10.1103/PhysRevB.54.11245.

[13] I. Gohberg, P. Lancaster, and L. Rodman, *Matrix Polynomials*, Academic Press, New York, 1982.

[14] G. H. Golub and C. F. Van Loan, *Matrix Computations*, The Johns Hopkins University Press, Baltimore, MD, 1996.

[15] J.-S. Guo, W.-W. Lin, and C.-S. Wang, *Numerical solutions for large sparse quadratic eigenvalue problems*, Linear Algebra Appl., 225 (1995), pp. 57–89, doi:10.1016/0024-3795(93)00318-T.

[16] T.-M. Huang, W.-J. Chang, Y.-L. Huang, W.-W. Lin, W.-C. Wang, and W. Wang, *Preconditioning bandgap eigenvalue problems in three dimensional photonic crystals simulations*, J. Comput. Phys., 229 (2010), pp. 8684–8703, doi:10.1016/j.jcp.2010.08.003.

[17] T.-M. Huang, H.-E. Hsieh, W.-W. Lin, and W. Wang, *Eigendecomposition of the discrete double-curl operator with application to fast eigensolver for three-dimensional photonic crystals*, SIAM J. Matrix Anal. Appl., 34 (2013), pp. 369–391, doi:10.1137/120872486.

[18] T.-M. Huang, H.-E. Hsieh, W.-W. Lin, and W. Wang, *Matrix representation of the double-curl operator for simulating three dimensional photonic crystals*, Math. Comput. Modelling, 58 (2013), pp. 379–392, doi:10.1016/j.mcm.2012.11.008.

[19] T.-M. Huang, H.-E. Hsieh, W.-W. Lin, and W. Wang, *Eigenvalue solvers for three dimensional photonic crystals with face-centered cubic lattice*, J. Comput. Appl. Math., 272 (2014), pp. 350–361, doi:10.1016/j.cam.2014.02.016.

[20] T.-M. Huang and W.-W. Lin, *A novel deflation technique for solving quadratic eigenvalue problems*, Bull. Inst. Math. Acad. Sin. (N.S.), 9 (2014), pp. 57–84.

[21] F. Hwang, Z. Wei, T.-M. Huang, and W. Wang, *A parallel additive Schwarz preconditioned Jacobi-Davidson algorithm for polynomial eigenvalue problems in quantum dot simulation*, J. Comput. Phys., 229 (2010), pp. 2932–2947, doi:10.1016/j.jcp.2009.12.024.

[22] T.-M. Hwang, W.-W. Lin, J.-L. Liu, and W. Wang, *Jacobi–Davidson methods for cubic eigenvalue problems*, Numer. Linear Algebra Appl., 12 (2005), pp. 605–624, doi:10.1002/nla.423.

[23] T.-M. Hwang, W.-W. Lin, and V. Mehrmann, *Numerical solution of quadratic eigenvalue problems with structure-preserving methods*, SIAM J. Sci. Comput., 24 (2003), pp. 1283–1302, doi:10.1137/S106482750139220X.

[24] T.-M. Hwang, W.-W. Lin, W.-C. Wang, and W. Wang, *Numerical simulation of three dimensional pyramid quantum dot*, J. Comput. Phys., 196 (2004), pp. 208–232, doi:10.1016/j.jcp.2003.10.026.

[25] E. Jarlebring, W. Michiels, and K. Meerbergen, *A linear eigenvalue algorithm for the nonlinear eigenvalue problem*, Numer. Math., 122 (2012), pp. 169–195, doi:10.1007/s00211-012-0453-0.

[26] E. Jarlebring and H. Voss, *Rational Krylov for nonlinear eigenvalues, an iterative projection method*, Appl. Math., 50 (2005), pp. 543–554, doi:10.1007/s10492-005-0036-9.

[27] J. D. Joannopoulos, S. G. Johnson, J. N. Winn, and R. D. Meade, *Photonic Crystals: Molding the Flow of Light*, Princeton University Press, Princeton, NJ, 2008.

[28] C. Kittel, *Introduction to Solid State Physics*, Wiley, New York, 2005.

[29] D. Kressner, *A block Newton method for nonlinear eigenvalue problems*, Numer. Math., 114 (2009), pp. 355–372, doi:10.1007/s00211-009-0259-x.

[30] C. Lee, *Residual Arnoldi Method: Theory, Package and Experiments*, Ph.D. thesis, TR-4515, Department of Computer Science, University of Maryland at College Park, College Park, MD, 2007.

[31] C. Lee and G. W. Stewart, *Analysis of the Residual Arnoldi Method*, Technical report, TR-4890, Department of Computer Science, University of Maryland at College Park, College Park, MD, 2007.

[32] R. B. Lehoucq, D. C. Sorensen, and C. Yang, *ARPACK Users' Guide: Solution of Large-Scale Eigenvalue Problems with Implicitly Restarted Arnoldi Methods*, SIAM, Philadelphia, 1998, doi:10.1137/1.9780898719628.

[33] B.-S. Liao, Z. Bai, L.-Q. Lee, and K. Ko, *Nonlinear Rayleigh-Ritz iterative method for solving large scale nonlinear eigenvalue problems*, Taiwanese J. Math., 14 (2010), pp. 869–883.

[34] M. Luo and Q. H. Liu, *Three-dimensional dispersive metallic photonic crystals with a bandgap and a high cutoff frequency*, J. Opt. Soc. Am. A Opt. Image Sci. Vis., 27 (2010), pp. 1878–1884.

[35] D. S. Mackey, N. Mackey, C. Mehl, and V. Mehrmann, *Vector spaces of linearizations for matrix polynomials*, SIAM J. Matrix Anal. Appl., 28 (2006), pp. 971–1004, doi:10.1137/050628350.

[36] V. Mehrmann and C. Schröder, *Nonlinear eigenvalue and frequency response problems in industrial practice*, J. Math. Ind., 1 (2011), 7, doi:10.1186/2190-5983-1-7.

[37] V. Mehrmann and H. Voss, *Nonlinear eigenvalue problems: A challenge for modern eigenvalue methods*, GAMM Mitt. Ges. Angew. Math. Mech., 27 (2004), pp. 121–152, doi:10.1002/gamm.201490007.

[38] E. Moreno, D. Erni, and C. Hafner, *Band structure computations of metallic photonic*

crystals with the multiple multipole method, Phys. Rev. B, 65 (2002), 155120, doi:10.1103/PhysRevB.65.155120.

[39] B. N. Parlett, *The Symmetric Eigenvalue Problem*, Prentice–Hall, Englewood Cliffs, NJ, 1980.

[40] A. Ruhe, *The rational Krylov algorithm for nonlinear matrix eigenvalue problems*, Zap. Nauchn. Semin. POMI, 268 (2000), pp. 176–180.

[41] K. Schreiber, *Nonlinear Eigenvalue Problems: Newton Type Methods and Nonlinear Rayleigh Functionals*, Ph.D. thesis, Institut für Mathematik, TU Berlin, Berlin, Germany, 2008.

[42] G. L. G. Sleijpen, A. G. L. Booten, D. R. Fokkema, and H. A. van der Vorst, *Jacobi-Davidson type methods for generalized eigenproblems and polynomial eigenproblems*, BIT, 36 (1996), pp. 595–633, doi:10.1007/BF01731936.

[43] G. L. G. Sleijpen and H. A. van der Vorst, *A Jacobi–Davidson iteration method for linear eigenvalue problems*, SIAM J. Matrix Anal. Appl., 17 (1996), pp. 401–425, doi:10.1137/S0895479894270427.

[44] D. B. Szyld and F. Xue, *Local convergence analysis of several inexact Newton-type algorithms for general nonlinear eigenvalue problems*, Numer. Math., 123 (2013), pp. 333–362, doi:10.1007/s00211-012-0489-1.

[45] F. Tisseur, *Backward error and condition of polynomial eigenvalue problems*, Linear Algebra Appl., 309 (2000), pp. 339–361, doi:10.1016/S0024-3795(99)00063-4.

[46] F. Tisseur and K. Meerbergen, *The quadratic eigenvalue problem*, SIAM Rev., 43 (2001), pp. 235–286, doi:10.1137/S0036144500381988.

[47] A. Vial, *Implementation of the critical points model in the recursive convolution method for modelling dispersive media with the finite-difference time domain method*, J. Opt. A: Pure Appl. Opt., 9 (2007), pp. 745–748, doi:10.1088/1464-4258/9/7/029.

[48] H. Voss, *An Arnoldi method for nonlinear eigenvalue problems*, BIT, 44 (2004), pp. 387–401, doi:10.1023/B:BITN.0000039424.56697.8b.

[49] H. Voss, *A Jacobi-Davidson method for nonlinear and nonsymmetric eigenproblems*, Comput. Struct., 85 (2007), pp. 1284–1292, doi:10.1016/j.compstruc.2006.08.088.

[50] W. Wang, T.-M. Hwang, W.-W. Lin, and J.-L. Liu, *Numerical methods for semiconductor heterostructures with band nonparabolicity*, J. Comput. Phys., 190 (2003), pp. 141–158, doi:10.1016/S0021-9991(03)00268-7.

[51] K. Yee, *Numerical solution of initial boundary value problems involving Maxwell's equations in isotropic media*, IEEE Trans. Antennas and Propagation, 14 (1966), pp. 302–307.

[52] Y. Zhao, C. Argyropoulos, and Y. Hao, *Full-wave finite-difference time-domain simulation of electromagnetic cloaking structures*, Opt. Express, 16 (2008), pp. 6717–6730, doi:10.1364/OE.16.006717.

[53] R. Ziolkowski, *Pulsed and CW Gaussian beam interactions with double negative metamaterial slabs*, Opt. Express, 11 (2003), pp. 662–681, doi:10.1364/OE.11.000662.